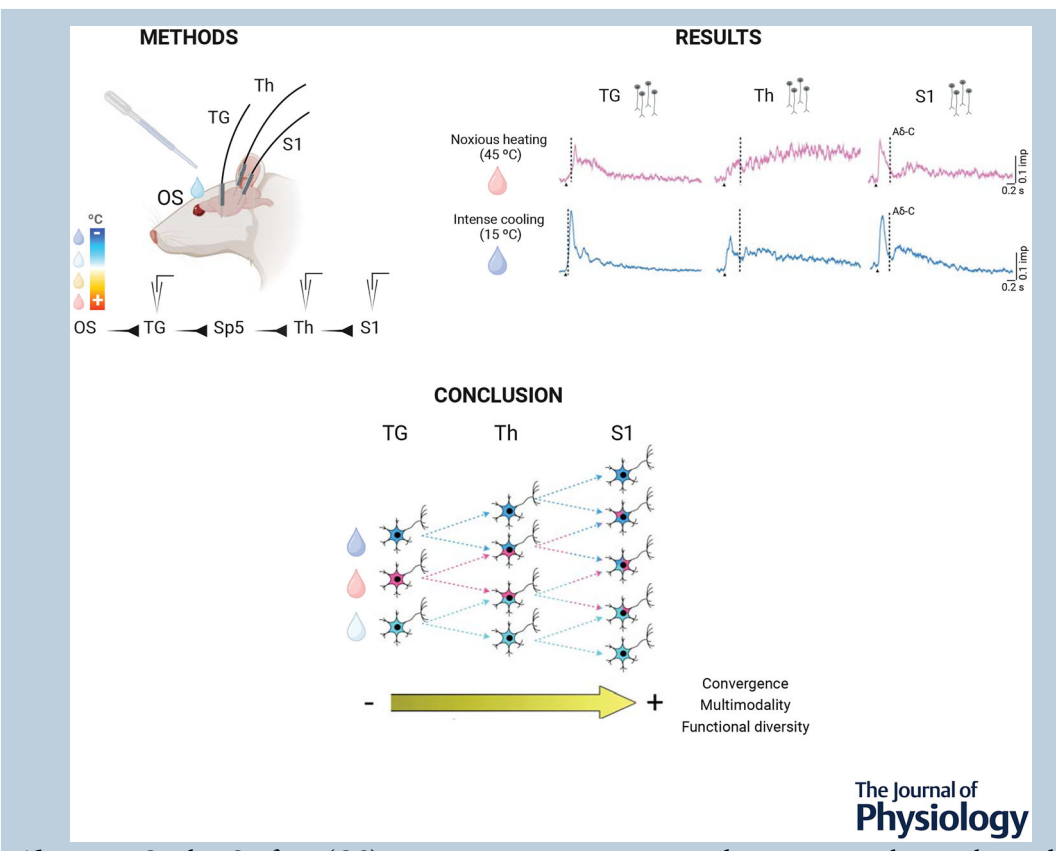
J Physiol 602.7 (2024) pp 1405–1426

Ocular surface information seen from the somatosensory thalamus and cortex

Enrique Velasco^{1,2,3,4}, Marta Zaforas^{5,6}, M. Carmen Acosta^{1,4}, Juana Gallar^{1,4,7} and Juan Aguilar^{5,6,8}

Handling Editors: Katalin Toth & Ilan Lampl

The peer review history is available in the Supporting Information section of this article (https://doi.org/10.1113/JP285008#support-information-section).



Abstract Ocular Surface (OS) somatosensory innervation detects external stimuli producing perceptions, such as pain or dryness, the most relevant symptoms in many OS pathologies. Nevertheless, little is known about the central nervous system circuits involved in these perceptions, and how they integrate multimodal inputs in general. Here, we aim to describe the thalamic and cortical activity in response to OS stimulation of different modalities. Electrophysiological extracellular recordings in anaesthetized rats were used to record neural activity, while saline drops at different temperatures were applied to stimulate the OS. Neurons were recorded in the

Check for updates

¹Instituto de Neurociencias, Universidad Miguel Hernández-CSIC, San Juan de Alicante, Spain

²Laboratory of Ion Channel Research, VIB-KU Leuven Center for Brain & Disease Research, Leuven, Belgium

³Neuroscience in Physiotherapy (NiP), Independent Research Group, Elche, Spain

⁴The European University of Brain and Technology, San Juan de Alicante, Spain

⁵Laboratorio de Neurofisiología Experimental, Unidad de Investigación, Hospital Nacional de Parapléjicos SESCAM, Toledo, Spain

⁶Instituto de Investigación Sanitaria de Castilla-La Mancha (IDISCAM), Spain

⁷Instituto de Investigación Sanitaria y Biomédica de Alicante, San Juan de Alicante, Spain

⁸Grupo de Investigación Multidisciplinar en Cuidados, Facultad de Fisioterapia y Enfermería, Universidad de Castilla-La Mancha, Toledo, Spain

ophthalmic branch of the trigeminal ganglion (TG, 49 units), the thalamic VPM-POm nuclei representing the face (Th, 69 units) and the primary somatosensory cortex (S1, 101 units). The precise locations for Th and S1 neurons receiving OS information are reported here for the first time. Interestingly, all recorded nuclei encode modality both at the single neuron and population levels, with noxious stimulation producing a qualitatively different activity profile from other modalities. Moreover, neurons responding to new combinations of stimulus modalities not present in the peripheral TG subsequently appear in Th and S1, being organized in space through the formation of clusters. Besides, neurons that present higher multimodality display higher spontaneous activity. These results constitute the first anatomical and functional characterization of the thalamocortical representation of the OS. Furthermore, they provide insight into how information from different modalities gets integrated from the peripheral nervous system into the complex cortical networks of the brain.

(Received 16 May 2023; accepted after revision 20 February 2024; first published online 8 March 2024)

Corresponding author J. Aguilar: Laboratorio de Neurofisiología Experimental, Unidad de Investigación, Hospital Nacional de Parapléjicos. SESCAM, C/ Finca La Peraleda. s/n. 45071 Toledo, Spain. Email: jdaguilar@sescam.jccm.es; J. Gallar: Instituto de Neurociencias, Universidad Miguel Hernández-CSIC, San Juan de Alicante, Spain. Email: juana.gallar@umh.es

Abstract figure legend Methods: Schematic depiction of the experimental approach, showing the use of several sensory modalities (intense cold, mild cooling, mild warmth and noxious heating) to stimulate the ocular surface (OS) during simultaneous electrophysiological recordings of the sensory pathway: trigeminal ganglion (TG), sensory thalamus (Th) and primary somatosensory cortex (S1). Results: TG, Th and S1 responses to the same stimulus modality are different in temporal profile and magnitude. Importantly, each sensory modality was processed in a different way inside the same structure of the sensory pathway, especially Th and Cx. Finally, the percentage of single neurons with multimodal responses was increased from the TG to Th, reaching higher in Cx. Conclusion: sensory modalities stimulating the OS are differently processed from the periphery (TG) to the central structures of the somatosensory system, Th and Cx, which showed increased complexity of response profiles and multimodal integration.

Key points

- Anatomical location of thalamic and cortical ocular surface representation.
- Thalamic and cortical neuronal responses to multimodal stimulation of the ocular surface.
- Increasing functional complexity along trigeminal neuroaxis.
- Proposal of a new perspective on how peripheral activity shapes central nervous system function.

Introduction

Sensory innervation of the ocular surface (OS) has been intensively studied due to its implication in many relevant physiological processes, as it transduces external stimuli and maintains corneal integrity, blinking and tearing homeostasis (Belmonte et al., 2004, 2017; Gallar

et al., 1993; González-González et al., 2017; Parra et al., 2010; Quallo et al., 2015). Traditionally, corneal innervation has been divided into three categories of peripheral receptors: mechanonociceptors detecting dangerous mechanical stimulus; cold-thermosensitive receptors activated by cold, reduced moistness, tear hyperosmolarity and silenced by warming; and

Enrique Velasco, better known as Quique, is a PhD and MSc in Neuroscience was originally educated as a physical therapist. His research has been centred on the functional study of the neural substrate for pain and somatosensation, from brain circuits to sensory neurons and ion channel biophysics, and is a specialist both in intra- and extracellular electrophysiology. Furthermore, he is a work leader from a group dedicated to the translation of basic neuroscience to the treatment of pain through physical therapies, such as electrical stimulation: the Neuroscience in Physiotherapy group (NiP).



14697793, 2024, 7, Downloaded from https://physoc.onlinelibrary.wiley.com/doi/10.1113/JP285008 by Readcube (Labtiva Inc.), Wiley Online Library on [23/05/2024]. See the Terms and Condition

(https://onlinelibrary.wiley.com/terms-and-conditions) on Wiley Online Library for rules of use; OA articles are governed by the applicable Creative Commons License

polymodal nociceptors detecting touch, chemical stimulation and noxious heating (Acosta, Belmonte et al., 2001; Acosta, Tan et al., 2001; Parra et al., 2010; Quallo et al., 2015). Accordingly, OS-related sensory perceptions include irritation, pain, freshness and dryness or gritty eyes. Moreover, aberrant OS sensory inputs due to accidental or surgical insults, such as cataract and photorefractive surgeries (Bech et al., 2018; Kovács et al., 2016; Luna et al., 2021; Piña et al., 2019), could induce chronic neuropathic symptoms, like trigeminal neuralgia, dry eye or pain (Gallar et al., 2004; Golan & Randleman, 2018; Kasetsuwan et al., 2013; Kato et al., 2019; Toda, 2018).

It has to be noted that, until now, research involving the OS sensory system has been centred mainly on the peripheral innervation of the OS, with minimal attention towards its central nervous system (CNS) representation. So far, CNS representation of the OS has only been studied in brainstem structures such as the principal and spinal trigeminal nuclei (Marfurt, 1981; Pozo & Cervero, 1993), in which functional changes produced by pathological states contribute to the symptom maintenance of chronic conditions, i.e. dry eye disease (Fakih et al., 2019; Rahman et al., 2015, 2017). Regarding the study of the functional responses of the brain to OS stimulation, the only available evidence is constituted by a promising case study, in which brain functional imaging was used to point towards the primary somatosensory cortex as a possible structure involved in OS-related human pain perception (Moulton et al., 2012).

This situation generates a gap of knowledge: it is unknown how information from the OS is computed in the brain. This gap is especially relevant from a translational point of view, as the characteristic aberrant sensory symptomatology produced in patients suffering from chronic pain pathologies have been related to plastic changes produced in thalamocortical networks (Guerrero-Moreno et al., 2020; Meacham et al., 2017; Sanzarello et al., 2016; Woolf, 1983). Nevertheless, the location, function and stimulus processing of thalamocortical networks receiving information from the OS are yet almost unexplored. Moreover, the capacity of the OS to detect many modalities of stimulation offers a good opportunity to use it as a model for the study of multimodal integration in the CNS.

Consequently, the aim of the present work is to functionally characterize the OS somatosensory representation in the CNS, including the peripheral ophthalmic branch of the trigeminal ganglion (TG), and the central somatosensory thalamus (Th) and primary somatosensory cortex (S1). For this purpose, we performed multi- and single-unit electrophysiological recordings in anaesthetized rats while stimulating the OS with stimuli of different modalities. Regarding results, we first report the stereotaxic coordinates at which

OS-responsive Th and S1 neurons can be recorded. Afterwards, a characterization of the neuronal responses of the TG, Th and S1 is described, both for population and single neurons, and for the diverse modalities of stimulation applied on the OS. Then we describe how multimodal integration and spatial organization of the single units are increased from the periphery towards the thalamocortical networks. Lastly, these results are discussed and compared with previously published evidence to frame their relevance, limitations and potential impact in future research.

Methods

Experimental model and ethical approval

Animal experiments conformed to the International Council for Laboratory Animal Science, European Union Regulation 2010/63/EU and were approved by the Ethical Committees for Animal Research of Hospital Nacional de Parapléjicos (Toledo, Spain) with code 177CEEA/2019 and Universidad Miguel Hernandez with code UMH.IN.JGM.03.20. They were carried out following the ARVO statement and ARRIVE guidelines for the use of animals in research. Healthy males from the Wistar rat strain (n=17) were used, weighing 250 to 400 g and with age between 2 and 4 months. All animals were housed in pairs, at 23°C on a 12 h light/dark cycle and *ad libitum* access to food and water.

Surgical procedures

Animals were anaesthetized using urethane (I.P. 1.5 g/kg) and placed in a stereotaxic frame (SR-6R; Narishige Scientific Instruments, Tokyo, Japan). Anaesthesia was kept constant at stage III-3 (Friedberg et al., 1999) during the entire experiment, using redosification if needed. Body temperature was kept constant at 36.5°C. Bilateral craniotomies were performed to access S1, Th and TG, following bregma-based coordinates from (Paxinos & Watson, 2007). Respect to the stimulated eye, ipsilateral TG, and contralateral Th and S1 were recorded.

Electrophysiological recordings

Extracellular recordings were performed using tungsten electrodes (2–5 $M\Omega$ impedance) (TM33B20KT and TM31C40KT, WPI, Inc., Sarasota, FL, USA). Recordings were amplified ($\times500$) and filtered in DC mode (0–3 kHz) using a preamplifier, filter and amplifier sequential circuit (Neurolog, Digitimer Ltd., Welwyn, UK). Analogue signals were converted to digital data at 20–50 kHz and with 64-bit quantization using a CED Power 1401 (Cambridge Electronic Design, Cambridge, UK,

RRID:SCR_01 6040) controlled by Spike2 software (v7.12; Cambridge Electronic Design, RRID:SCR_000903).

To record TG neurons, we used the stereotaxic coordinates for neurons innervating OS, previously defined by our research group: AP = -1.5, ML = 2, DV = 10 mm. Since the stereotaxic coordinates of OS neurons in the thalamus and S1 had not been described yet, we used those of periocular tissues described by Chapin & Lin (1984) for S1, and by Diamond, Armstrong-James, Budway et al. (1992) and Diamond, Armstrong-James, Ebner et al. (1992) for the thalamus as a

starting screening point (Fig. 1*A*). Again, recordings were contralateral for S1 and Th, and ipsilateral for TG with respect to the stimulated eye. After recording from one eye in an animal, we switched stimulation and electrodes to record the responses of the other eye. The total numbers of electrophysiological recordings were 17 in S1, 15 in Th and eight in TG (Fig. 1*B*).

To identify units receiving OS information, once a firing neuron was recognized in the recording, whiskers, eyebrows, eyelid borders and the cornea were mechanically stimulated using a fine brush. To further 14697793, 2024, 7, Downloaded from https://physoc.onlinelibrary.wiley.com/doi/10.1113/JP285008 by Readcube (Labtiva Inc.), Wiley Online Library on [23/05/2024]. See the Terms

inditions) on Wiley Online Library for rules of use; OA articles are governed by the applicable Creative Commons License

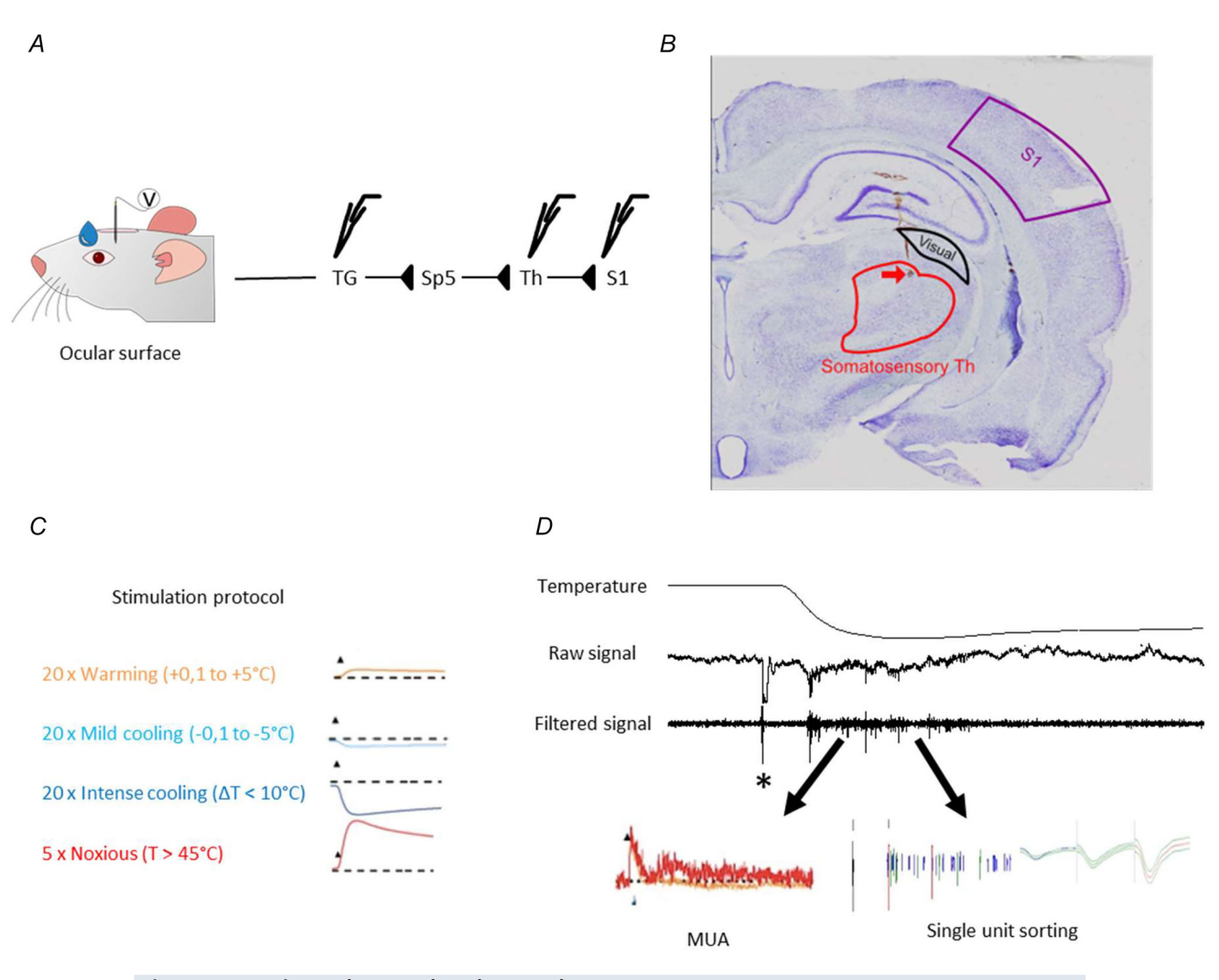


Figure 1. Experimental approach and protocol

A, schematic representation of the experimental configuration for stimulation and electrical recording over the canonical ocular surface (OS) sensory pathway. B, coronal brain slice of one of the rats used for thalamic recordings, showing the electrode's track reaching the edge between ventral posteromedial (VPM) and posteromedial (POm) thalamic nuclei. In these areas, ocular surface-evoked activity was successfully recorded. The delimited red and black areas account for the somatosensory and visual thalamus, respectively. C, stimulation protocol showing the temperature change produced by each type of stimulus used in this study. The dotted line represents the basal ocular surface temperature of the rat (28–32°C). D, example of an electrophysiological recording of S1 activity and its processing, showing the response to an intense cold stimulus (the upper trace corresponds to OS temperature). A filtering and sorting protocol were applied to obtain values of multiunit (MUA) and single-unit activity. The artefact (*) produced by the drop contacting the eye was used as a proxy for stimulus onset, averaging and latency calculation. [Colour figure can be viewed at wileyonlinelibrary.com]

4697793, 2024, 7, Downloaded from https://ptlysoc.onlinelibrary.wiley.com/doi/10.1113/P285008 by Readcube (Labtiva Inc.), Wiley Online Library on [23/05/2024]. See the Terms and Conditions (https://onlinelibrary.wiley.com/error

and-conditions) on Wiley Online Library for rules of use; OA articles are governed by the applicable Creative Commons License

confirm whether a given unit was innervating the OS, and to be able to detect non-mechanosensitive units, a drop of ice-cold saline (0.9%, B. Braun) was applied over it. Noxious stimulation was not used for the screening to avoid damage to the OS.

Ocular surface stimulation

The OS stimulation consisted of the topical application of 20 μ L saline (0.9%, B. Braun) drops at different temperatures (range 10–60°C, inducing OS temperature changes between -20° and $+30^{\circ}$ C, respect to a basal OS temperature of 30°C), with 30 s intervals between stimuli. A calibrated Pasteur pipette with thin tip was used to deliver the saline drops used as stimulus across all experiments and animals. In order to avoid additional mechanical stimulation from the drop falling from a high altitude, the pipette was manually pressed until the drop hung from the tip and approximated to the OS.

OS temperature was constantly monitored using a high-speed thermal microprobe in contact with the cornea (Clifton, NJ, USA). We used this probe to measure how much the temperature of the OS changed when stimulated, from its basal temperature to the maximum or minimum temperature reached when hot or cold drops were applied, respectively. This variable was called peak temperature change (ΔT). Then, thermal stimuli were divided into four categories according to their ΔT : *intense cold* (ΔT greater than -10° C), *mild cooling* (ΔT between -0.1 and -5°C), mild warmth (Δ T between +0.1 and +5°C) and noxious heating (at least $\Delta T +11$ °C, reaching a final temperature above 40°C) (Vandewauw & Voets, 2016). At least 20 stimuli of each category were performed in every recording and averaged for analysis. The only exception was noxious heating stimulus, in which five drops were applied, waiting 5 min between them to minimize sensitization and damage to the OS. Stimuli were always applied in the same order described here, from the mildest to the most hazardous: mild cooling → mild warmth \rightarrow intense cold \rightarrow noxious heating (Fig. 1*C*).

Data analysis

Multiunit activity analysis. To identify neuronal activity, raw signals were first digitally filtered (0.3–3 kHz). Then, a threshold for spike detection was set at $2.576 \times SD$ (99% CI) away from background noise. The resulting signal was termed multiunit activity (MUA), which corresponds to the extracellular action potential activity of all the recorded population (Fig. 1*D*).

The MUA signal was analysed following a previously established division in $A\beta$, $A\delta$, C and post-discharge components (Castro et al., 2017). Considering a 2 cm distance between the OS and the TG, and the

conduction velocities (CVs) previously reported for trigeminal sensory neurons (Pinto et al., 2008), no $A\beta$ responses were detected in our recordings. This is consistent with previous reports of the OS lacking heavily myelinated, fast-conducting fibres to avoid impairing the required transparency of the cornea (López de Armentia et al., 2000; Müller et al., 2003). Coherently, our data displayed A δ , C and post-discharge components, but as C and post-discharge were frequently fused in a single component, we pulled them together for analysis. Therefore, our responses were divided into two components: the first component in the range of A-fibre latencies (mainly $A\delta$); and the second component representing neuronal activity with longer latencies due to the slower conduction velocity of C-fibres and post-discharge.

Considering the CV ranges described for different axonal types, we calculated the corresponding ranges of latencies for the distance between OS and the TG (2 cm). As result, for the $A\delta$ fibres activation (CV range: 1.8–17.4 m/s), neurons in the TG were activated in a latency range of 1–11 ms; while for the C-fibre activation (CV range: 0.34–1.3 m/s), the neurons in the TG were activated in a latency range of 15–59 ms. Therefore, the TG latency cutoff between the first and the second components was set at 15 ms.

To calculate the latencies of the response in the Th, we took the response latencies previously obtained for TG, and added the antidromic conduction latencies between the trigeminal nucleus in the brainstem and the thalamus reported by Minnery and Simmons (2003), plus 1 ms to account for the synaptic crossing and action potential firing. Finally, to calculate the latencies to the responses in S1, 2 ms were added to account for the extra synapse and the thalamocortical projection. This rendered a cutoff between the first and second components of 33 and 35 ms for Th and S1, respectively. Components were then analysed for peak amplitude and peak latencies.

Single-unit activity analysis. To isolate single neuron activity, we applied a spike-sorting protocol based on templates over the MUA recording. Said templates were built based on waveform shape coincidences. This spike sorting was conducted by homemade scripts using semi-automated Spike 2 software and Python Anaconda (Spyder, RRID:SCR_01 7585) (Rossum & Drake, 2009) (Fig. 1*D*). A total of 219 single units were extracted from the different recording locations as follows: 49 from TG recordings, 69 from Th and 101 from S1.

Peristimulus time histograms (PSTH) were constructed to characterize the single-unit responses against different modalities of stimuli. A response was determined as positive if the PSTH showed at least 1 ms bin displaying a value $2.576 \times SD$ (99% CI) away from the mean

basal activity in the 2 s prior to stimulation, and then manually confirmed by the experimenter to avoid random detections of a single bin response. For units with very low firing rates, to avoid having only bins with values of 0 and 1 impulses, the bin size was increased to 5 ms. Afterwards, each neuron was tagged depending on the specific combination of such modalities (mechanical, warming, noxious and cold). For example, a neuron responding to the mechanical stimulus due to the drop contact on OS, but unaffected by different temperatures applied was tagged as mechanosensitive; a neuron with this response, but also responding to noxious stimulation was identified as responsive to mechanical and noxious stimulus.

Statistics

The software used were SPSS v25 (IBM Corporation, RRID:SCR 0 02865) and Excel (Microsoft Corporation, RRID:SCR_01 6137). Quantitative comparisons between two independent neurons or recording sites were performed with independent t tests. For comparisons within the same recording site, a paired t test was used. To compare more than one group, one-way ANOVA with a Bonferroni post hoc correction was used. When the Shapiro-Wilk test and manual inspection of the histogram and density curves clearly revealed a non-normal distribution, equivalent non-parametric tests (Mann-Whitney's U test, Wilcoxon's, and Kruskal-Walliss with Bonferroni post hoc corrections over Mann-Whitney's U, respectively) were used. For comparing the percentage of units displaying variable or constant response dynamics, Fisher's exact test was employed. Responses to repeated stimulation were averaged within recording sites for MUA analysis, and within neurons for single-unit analysis. Therefore, data points represent a single neuron/recording site, constructed by averaging all the stimuli applied in that recording.

Results

The OS is represented in the sensory thalamus and the primary somatosensory cortex

Thalamic OS responses were located ventrally with respect to the dorsolateral geniculate nucleus (dLGN) and in the proximity of α and β vibrissae somatotopic representations (Clemens et al., 2018) (Fig. 2A). Indeed, while lowering the electrode, responses to light and mechanical stimulation were used to ascertain the dorsal and ventral limits for OS representation, respectively: when responses to visual stimulation disappeared, usually responses to OS stimulation appeared (Fig. 2B-C). In

summary, the OS representation was found to be medial and ventral with respect to visual responses. The thalamic coordinates in which we found responses towards OS stimulation were (from bregma): AP - 3.5 to -4 mm; ML 3 to 4 mm; DV 4.2 to 5.1 mm (1/17 at DV 5.7), corresponding to the most dorsal part of the border separating the posterior medial complex of thalamus (POm) from the ventral posteromedial nucleus (VPM), with recording locations distributed in both nuclei (Fig. 2A-B).

In S1, the well-known cortical whisker representation of V2 trigeminal branch innervating the middle face is caudal to that of trigeminal V3 branch innervating the jaw and lower face (Deschênes et al., 2005; Furuta et al., 2009). Following this logic, the representation of trigeminal V1 (ophthalmic and upper face) should be located caudal to V2 in the somatosensory cortex, near the representation of α and β whiskers. This was indeed the case (Fig. 2*D*), and for S1 the stereotaxic coordinates in which we recorded OS-sensitive neurons spanned AP 3.7–5.7 mm; ML 5.2–7.2 mm; DV 0.32–1.4 mm (Fig. 2*E*). The majority of our cortical recordings were located in the deep IV and V layers, with only one recording in layer II/III (Fig. 2*E*).

The modality of the stimulation is encoded by CNS neurons in different time components of the response

14697793, 2024, 7, Downloaded from https://physoc.onlinelibrary.wiley.com/doi/10.1113/JP285008 by Readeube (Labtiva Inc.), Wiley Online Library on [23/05/2024]. See the Terms and Conditions (https://onlinelibrary.wiley.com/erms-and-conditions) on Wiley Online Library for rules of use; OA arctices are governed by the applicable Creative Commons Licensers

Next, we characterized the physiological responses elicited by OS sensory stimulation using drops with four different thermal ranges: warmth, noxious heating, mild cooling and intense cold. For this purpose, we analysed the averaged neuronal population responses, based on the MUA from each recording location in all three studied structures TG, thalamus and S1.

Mild warmth drops induced a response consisting in a fast and transient increase of the firing rate in all recorded structures, with latencies falling within A-δ ranges (Fig. 3A). Moreover, this component presented similar amplitude, latency and duration regardless of the temperature of the drop applied (P > 0.05; ANOVAs of repeated measurements) (Table 1). Considering previous studies on corneal receptors showed that there are no warmth receptors in the OS (Gallar et al., 1993; González-González et al., 2017), and latencies of the response are coherent with the mildly myelinated A- δ mechanosensitive fibres of the OS (López de Armentia et al., 2000; Müller et al., 2003), we assume that this first component is a mechanical response towards the saline drop touching the eye, equally present in all stimulation modalities.

Noxious heating induced a response with a first and second component in Th and S1 (to the left and right of the vertical dotted line within each trace, respectively,

14697793, 2024, 7, Downloaded from https://physoc.onlinelibrary.wiley.com/doi/10.1113/JP285008 by Readcube (Labtiva Inc.), Wiley Online Library on [23/05/2024]. See the Terms

conditions) on Wiley Online Library for rules of use; OA articles are governed by the applicable Creative Commons I

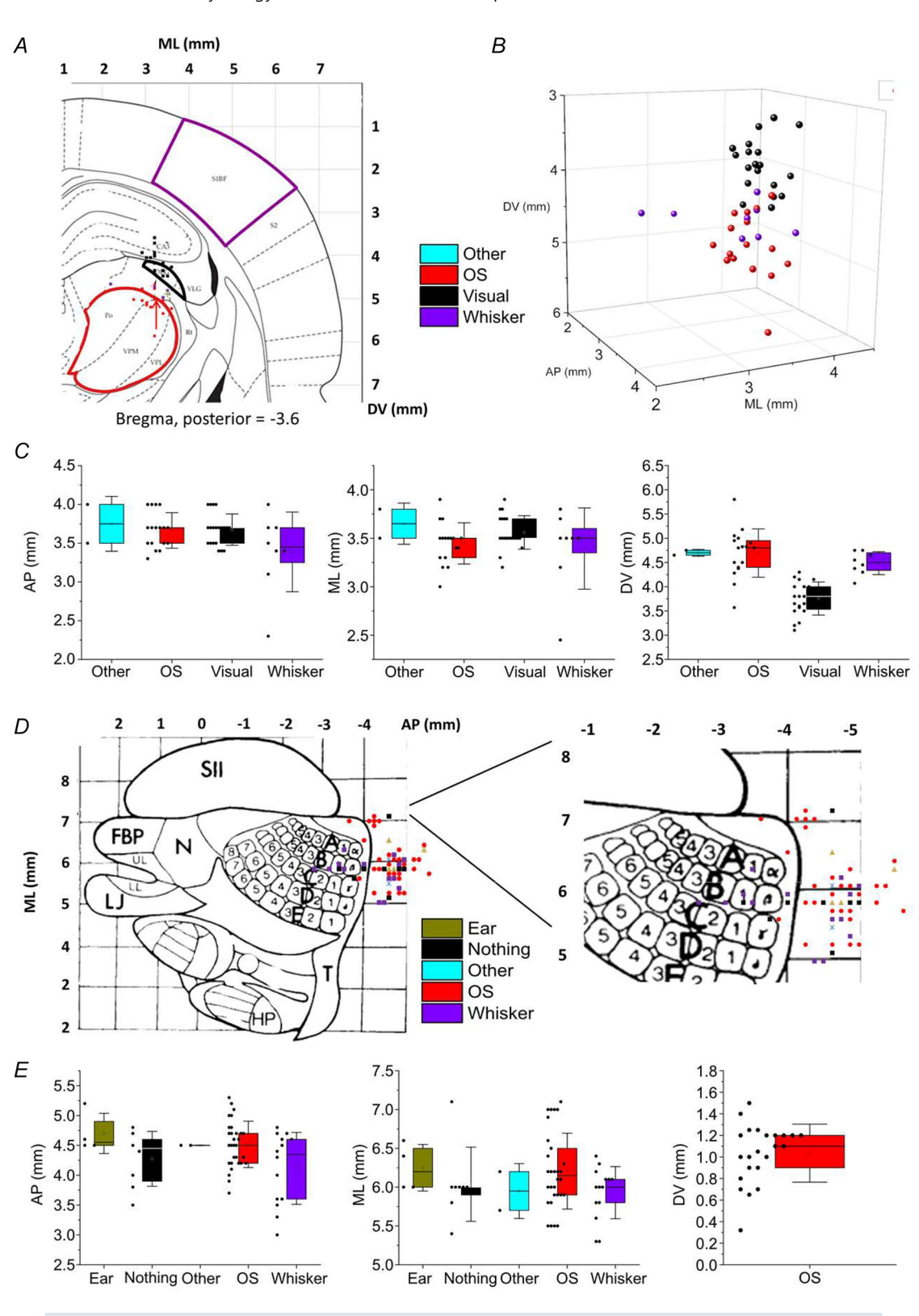


Figure 2. Ocular surface somatosensory representation in the sensory thalamus and primary somatosensory cortex (S1)

Thalamic recording sites coordinates are represented on a frontal schema (A), in a 3D projection (B) and for each individual axis (C). S1 coordinates represented schematically from above (D and inset) and for each individual axis

(E). The delimited dark red and black areas account for the somatosensory and visual thalamus, respectively, while the red arrow in A represents the average coordinates in which OS activity was found. Schemes of the thalamus and brain primary somatosensory brain cortex are from Paxinos & Watson (2007) and Chapin & Lin (1984), used with permission of the copyright holders. Other = category comprised paws, trunk, tail and facial areas not included in the other categories. Box plots of C and E indicate median (line), percentiles 25 and 75 (box range) and SD (whiskers). Number of recording coordinates (N): Th = 48, S1 = 58, from 17 animals. [Colour figure can be viewed at wileyonlinelibrary.com]

in Fig. 3*B*). As previously described, the first component was the response to the mechanical stimulation of the drop, which showed a peak latency within the A- δ range. Moreover, the second component, which was never observed for warmth stimulation, showed a delayed latency for the peak of response in all nuclei (P < 0.001, paired t test, Table 1). In the first place, recorded TG responses to noxious heating stimulation presented slow latencies, falling in the C-fibre range (114 (58) ms, see Fig. 3*B*). Coherently, the second component of Th and

S1 responses showed consistently delayed latencies 726 (277) and 302 (57) ms, respectively; Fig. 3B; Table 1. Our interpretation of these results is that while in the case of TG responses the first component was due to activation of A δ -fibres encoding mechanical stimulation of the drop, the second component is generated by C-fibre activation, which encoded the noxious heat information of the stimulus. This assumption is based, on the fact that polymodal nociceptors detecting noxious heat in the OS have slower CVs than mechanosensitive fibres

14697793, 2024, 7, Downloaded from https://physoc.onlinelibrary.wiley.com/doi/10.1113/JP285008 by Readcube (Labtiva Inc.), Wiley Online Library on [23/05/2024]. See the Terms and Conditions (https://onlinelibrary.wiley.a

and-conditions) on Wiley Online Library for rules of use; OA articles are governed by the applicable Creative Commons License

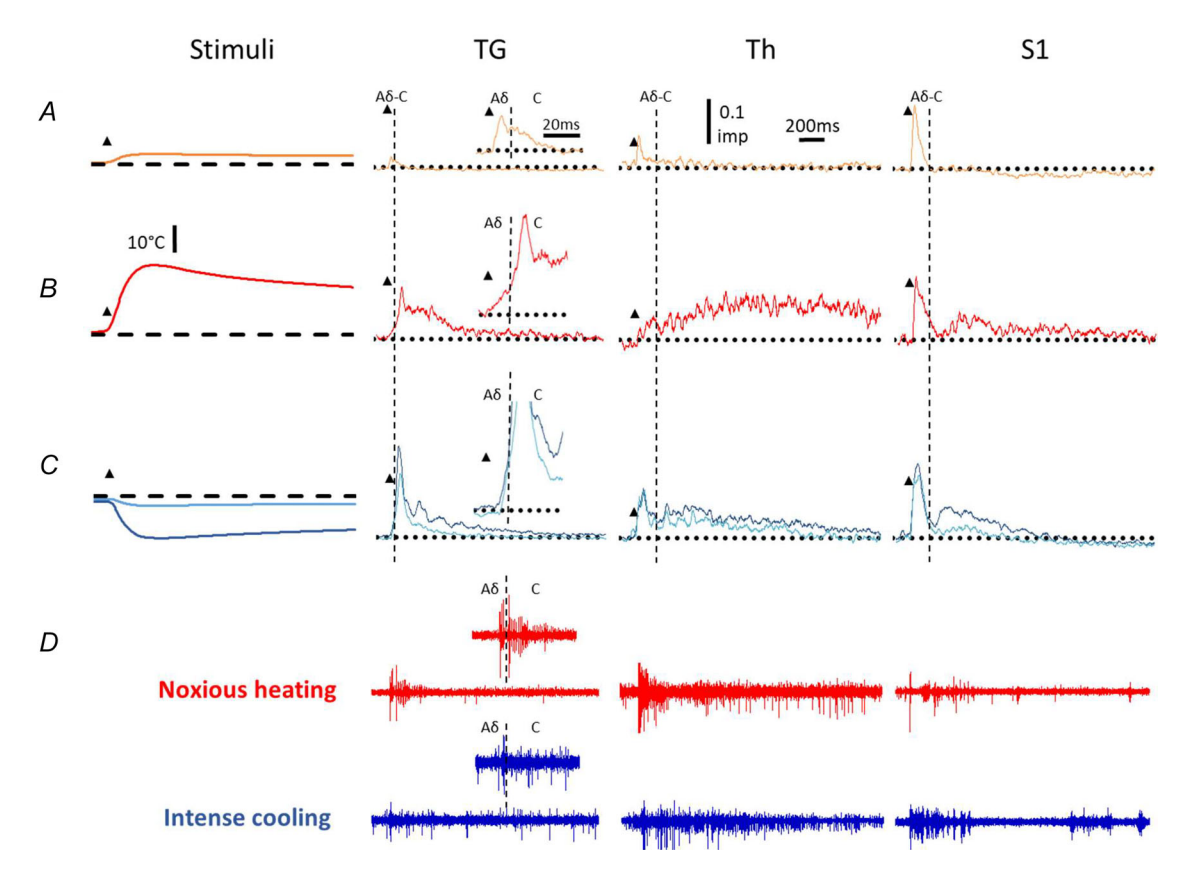


Figure 3. The modality of the ocular surface stimuli is encoded in the central nervous system response components

A, temperature traces produced by warmth stimulation and averaged multiunit activity (MUA) responses evoked at the trigeminal ganglion (N = 8 recording sites); the somatosensory thalamus (N = 15 recording sites); Somatosensory cortex (N = 17 recording sites), from 17 animals). B - C, same for noxious heating and mild/intense cooling. Each average was calculated with the response to 15–20 stimuli in each recording site using 1 ms bins, except for noxious heating in which only five stimuli were employed. For a better visualization, a sliding average of 20 ms was applied to the traces. Black triangles mark the artefact produced by the instillation of the stimulation drop, used as time zero. The insets represent a zoom in of the trigeminal responses, with the latency cutoff between the part of the response that is attributable to the A- and C-fibre-evoked response represented as a dotted line. D, representative individual MUA recordings performed at each structure showing the responses to noxious heat (red traces) and intense cold stimulation (blue traces). [Colour figure can be viewed at wileyonlinelibrary.com]

Table 1. Characteristics of the multiunit activity (MUA) response of neurons recorded in the trigeminal ganglion (TG), thalamus (Th) and primary somatosensory cortex (S1) to different thermal stimuli.

		First component				Second component		
		Mild warmth	Noxious heat	Mild cooling	Intense cold	Noxious heat	Mild cooling	Intense cold
TG (V1)	Peak (imp/ms)	0.13 ± 0.1	0.13 ± 0.1	0.13 ± 0.1	0.14 ± 0.1	0.62 ± 0.2	0.42 ± 0.2	0.53 ± 0.2
	Latency (ms)	9.4 ± 3.8	7 ± 3.5	8.1 ± 4.1	$\textbf{7.8} \pm \textbf{2.4}$	114 ± 58	56 ± 20.4	52 ± 16
Th	Peak (imp/ms)	$\textbf{0.21} \pm \textbf{0.1}$	$\textbf{0.31} \pm \textbf{0.1}$	$\textbf{0.25} \pm \textbf{0.1}$	0.20 ± 0.1	$\textbf{0.52} \pm \textbf{0.2}$	$\textbf{0.30} \pm \textbf{0.1}$	$\textbf{0.30} \pm \textbf{0.2}$
	Latency (ms)	20.9 ± 5.5	21.8 ± 5.3	21.9 ± 7.3	19.6 ± 5.7	726 ± 277	121 ± 104	138 ± 144
S1	Peak (imp/ms)	$\textbf{0.23} \pm \textbf{0.1}$	$\textbf{0.41} \pm \textbf{0.1}$	$\textbf{0.23} \pm \textbf{0.1}$	0.21 ± 0.1	$\textbf{0.45} \pm \textbf{0.2}$	0.19 ± 0.1	0.23 ± 0.1
	Latency (ms)	24.7 ± 6	24.5 ± 6.1	25.8 ± 6.1	26.5 ± 5.8	302 ± 57	297 ± 60	278 ± 74

Latency, in ms, represents the time from the stimulus initiation to the peak of the response. Data are presented as means \pm SD. N: TG = 8 recording sites; Th = 15; S1 = 17, from 17 animals.

(Gallar et al., 1993; Rivera et al., 2000). This same result was confirmed for our data set (Fig. 4). Regarding the responses observed in Th and S1, the long latencies observed for the second component could be either attributed to the slow CVs of non-myelinated OS afferents (López de Armentia et al., 2000; Müller et al., 2003), to a potential transmission of the information through the paralemniscal pathway, which is slower and has been described to convey noxious information in other tissues

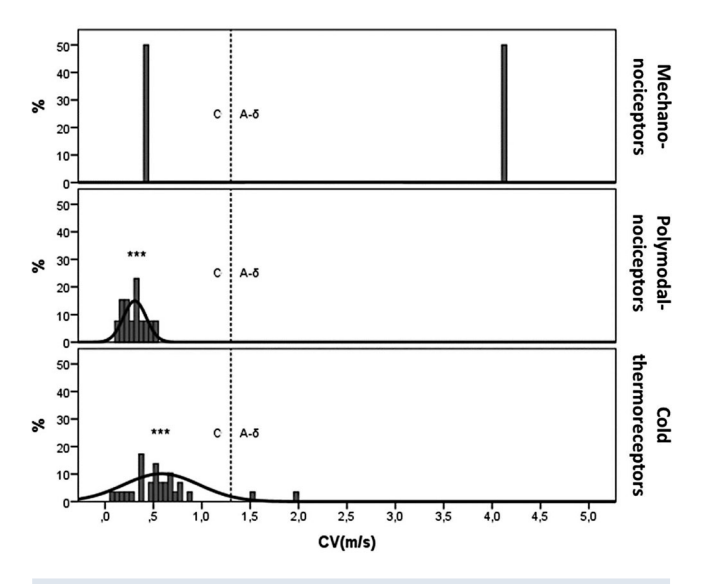


Figure 4. Conduction velocity of the different functional types of ocular TG neurons

Conduction velocity (CV, in m/s) of the peripheral axons of TG neurons innervating the ocular surface was calculated from the latency between the onset of the stimulus and the moment of their positive response, and the distance travelled. Considering the homogeneous size of the animals, a fixed distance of 20 mm from OS nerve ending to TG soma was used for the calculation. CVs of nociceptive TG neurons belong to the C range and were significantly lower than CVs of cold-thermosensitive trigeminal ganglion neurons (***P < 0.01, independent t test), which included C and A-fibres. Despite the low number of recorded pure mechanosensitive neurons, both C and A were found.

(Diamond, Armstrong-James, Ebner et al., 1992; Mo et al., 2017), or to a combination of both. This was particularly clear in the thalamus, where the second component lasted well beyond 1 s after stimulation.

Mild cooling and intense cold stimulation also produced a second component in Th and S1 responses, consistent with the C-fibre latencies observed in the TG responses (Fig. 3C, Fig. 4). The latency of the second component was faster for cold responses than for noxious heating responses in all structures, reaching significance in TG (52 (16) vs. 114 (58) ms, respectively; P = 0.009) and Th (138 (144) vs. 726 (277); P < 0.001) but not in S1 (278 (74) vs. 302 (57); P = 0.294) (Table 1, Fig. 3D). This is again in agreement with the CVs of peripheral nerve fibres for TG responses, as cold receptors are faster than nociceptors detecting noxious heat (Gallar et al., 1993). This cold-evoked second component presented higher amplitude for intense cold than for mild cooling in TG (0.53 (0.2) vs. 0.42 (0.2) imp/ms, respectively; P = 0.036,paired t test) but not in Th (0.30 (0.2) vs. 0.30 (0.1); P = 0.911) nor S1 (0.23 (0.1) vs. 0.19 (0.1); P = 0.154) (Table 1).

Single neurons from the CNS receive multimodal inputs, producing different response dynamics

Next, we analysed the response of single units to decipher whether they have a homogeneous behaviour in response to different stimulation modalities, or if they show different response profiles that contribute to the creation of the populational response. Our main finding is that Th and S1 single neuron responses followed one of three different dynamics: (A) bimodal responses, displaying both an initial $A\delta$ and a second C component; (B) initial-only responses, presenting exclusively the $A\delta$ component; (C) second-only responses, presenting solely the late C component. This finding demonstrates that the population responses based on MUA are composed by the

summation of different response dynamics of single units. Examples of each type are illustrated in Fig. 5*A*.

We went one step further, characterizing each single-unit response profile depending on the stimulation modality. Interestingly, we found that most of the units showed different response dynamics depending on the stimulus applied instead of a constant response dynamic (Fig. 5B, upper charts). In this way, most single neurons could show at least two of the three profiles described above depending on the modality of stimulation. For example: when a heating stimulation is applied, a single neuron could respond with only the first component to warmth stimulation, but if the heating was more intense (noxious heating) the neural response exhibited a bimodal profile with two components. In fact, most units showed different response dynamics towards warmth and noxious heating stimulation (Fig. 5B, middle charts). In contrast, the proportion of variable responses was smaller when comparing mild and intense cold responses, both in S1 and Th (P = 0.001 and P < 0.001, respectively; Fisher's exact test) (Fig. 5B, lower charts). These results indicate that the same unit can respond differently in function of the combination of the modalities activated. Therefore, single neurons in the somatosensory Th and S1 have the capacity to discriminate in their responses the modality of stimulus applied over the OS, rather than simply detecting that the OS has been stimulated without carrying modality information. Finally, populational Th responses to noxious heating were strikingly long lasting, as previously described (Fig. 3B). At the single-unit level the underlying mechanism for this constant response was revealed: a prolonged recruitment of new units into the response, with the last neurons being activated as late as ~600 ms after stimulation of the OS (data not shown). The long-lasting activation and new units observed in Th after nociceptive stimulation could be due to the cholinergic action that is triggered by nociceptive stimulation. We consider that the cholinergic activation could be responsible for the 'post-discharge' described in Castro et al. (2017), and physiologically explained by Castro-Alamancos & Oldford (2002) and Castro-Alamancos (2004). In our work, this new long-lasting recruitment due to noxious heat stimulation was considered part of the second component, and it contributes to displace the latency to peak of the second component response far from the onset latency of the second component.

Next, for each individual neuron, we compared the specific response produced by warmth stimulation towards the response to noxious heating specifically, in Th (Fig. 5C) and S1 (Fig. 5D), to analyse how the nociceptive modality is being encoded by comparing a non-noxious stimulation (the mechanically elicited response of the warmth drop) towards a noxious heating stimulation. As these graphs show, the majority of

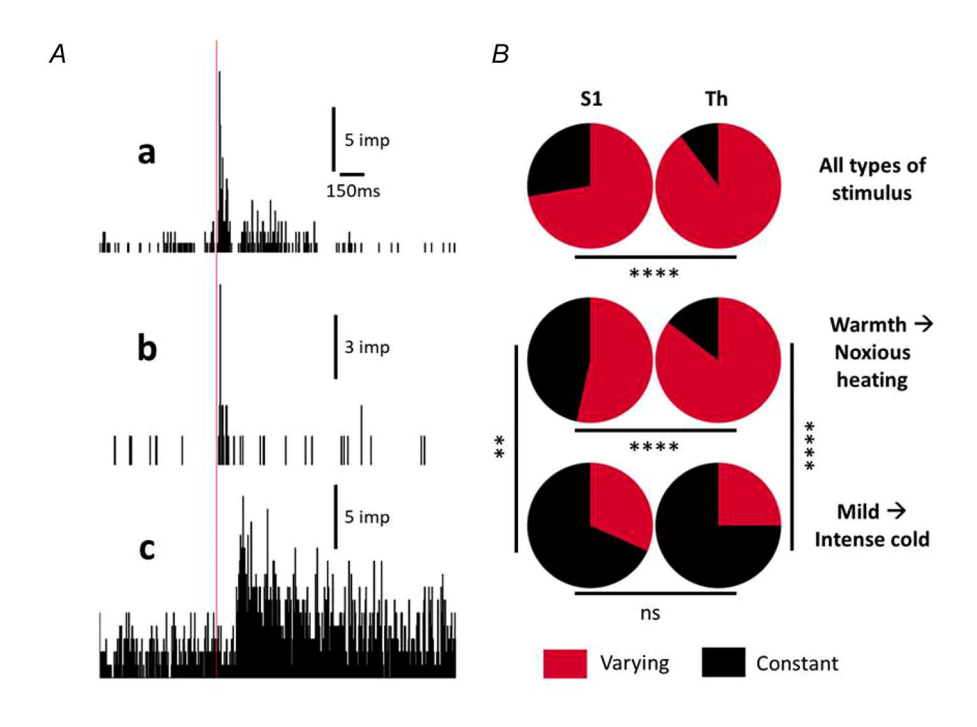
'varying responses' are neurons with an 'initial-only' response type towards warmth stimulation (a mechanical response), adopting a 'bimodal' or 'second-only' response when challenged with noxious heating. In fact, neurons responding to the warmth drop with an initial-only component (mechanical response), and then displaying a bimodal response to noxious heating (mechanical A + noxious heating C responses) can be considered as wide dynamic range neurons (WDR) encoding both noxious and non-noxious stimulation, using classical terminology. In contrast, some neurons unresponsive to warmth are activated by noxious heating, adopting a 'second-only' response type. This latter group can be considered as specific high threshold nociceptive neurons, in contrast to WDR units.

CNS neurons that respond to OS stimulation have greater multimodality, exhibiting more diverse functional populations than in peripheral neurons

As the previous results indicate, the single-unit responses are not homogeneous or uniform across stimulation modalities. This could be due to convergence of different sensory pathway inputs into the same unit. To test this hypothesis, each single TG, Th and S1 neuron was classified between 0 and 4, representing how many sensory modalities of stimulation (mechanical, warming, noxious and cold) they were responsive to. Therefore, a neuron with a 4 is a neuron responding to every sensory modality. Furthermore, the specific combination of four stimulus modalities allows a maximum of 16 theoretical identities of functional populations (4²).

14697793, 2024, 7, Downloaded from https://physoc.onlinelibrary.wiley.com/doi/10.11131/P285080 by Readcube (Labtiva Inc.), Wiley Online Library on [23/05/2024]. See the Terms and Conditions (https://onlinelibrary.wiley.com/terms-and-conditions) on Wiley Online Library for rules of use; OA articles are governed by the applicable Creative Commons Licenson

As a first result, the units were increasingly multimodal along the somatosensory axis (TG<Th<S1; see Fig. 6A), i.e. a higher percentage of neurons were responsive to an increased combination of stimulation modalities. In the TG, units belonging to 7 out of 16 functional types were found (Fig. 6B), predominantly the units responding both to cold and noxious stimulation (\sim 45%). This profile could be explained by previous work (Acosta et al., 2014; Belmonte et al., 2017), being 32% of these neurons identified as polymodal nociceptors, and 68% as cold thermoreceptor neurons with paradoxical response to noxious heating. Overall, TG results coincide with previous reports stating that the OS is innervated mainly by polymodal nociceptors and cold receptors, with a minor contribution of mechanosensitive receptors and a lack of warmth receptors (Belmonte et al., 2017; González-González et al., 2017). The analysis of thalamus showed increased complexity of single neuron responses by reaching 9 out of 16 different functional types, still with the cold-noxious type predominant (Fig. 6B). Finally, the higher complexity was observed in S1 single neuron responses, with a diversity reaching 14 out 16 functional



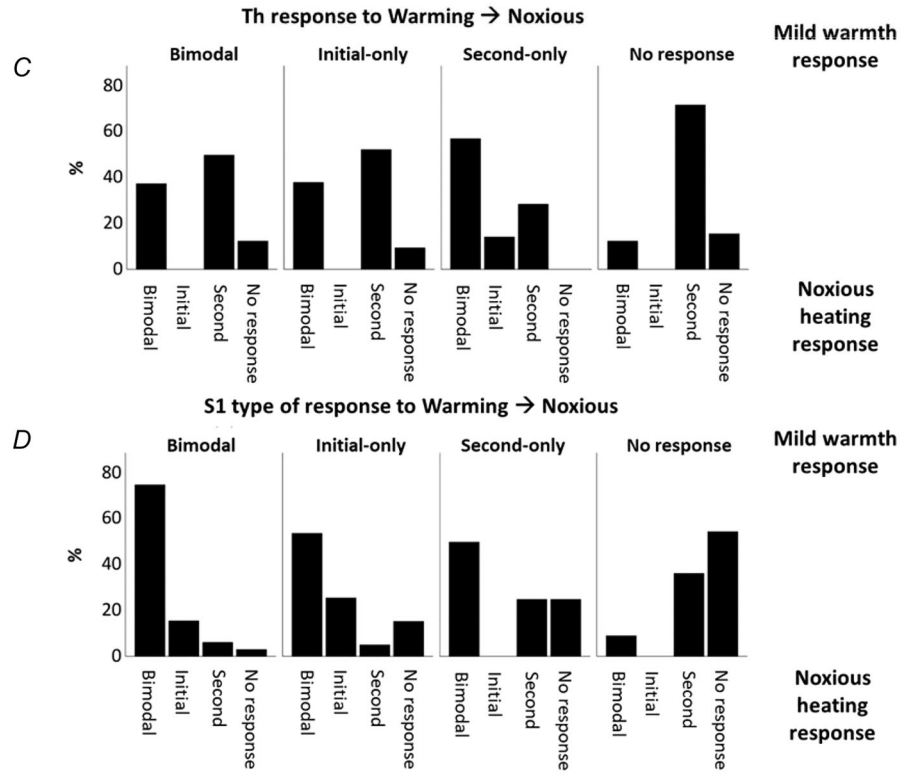


Figure 5. Response dynamics of single units in the Th and S1 ocular surface representations A, representative peristimulus time histograms of the dynamics of the response to intense cold stimulation of three different S1 units: bimodal response (a), initial-only (b), second-only (c), components. B, percentage of S1 and Th units with the same (Constant) or different types of response (Variable) to warming and noxious stimulation, intense and mild cooling. (**P < 0.01; ****P < 0.0001, Fisher's exact test). C, distribution of response dynamics to warming and noxious stimulation of the same unit. Each unit was first classified as bimodal, initial-, second-only, or no response according to its type of response to warming stimulation (upper labels dividing panels); then, the dynamics of the response of each unit to noxious stimulation was represented (x-axis labels). x: TG = 49 single units; Th = 69; S1 = 101. Single units were isolated from 17 recording sites in S1, 15 in Th and 8 in TG, from a total of 17 animals. [Colour figure can be viewed at wileyonlinelibrary.com]

types, including units responsive to the four types of stimuli (Fig. 6B).

Interestingly, although no peripheral neurons were warmth-sensitive, we found neurons encoding warmth stimulation in the second component of their responses both in Th and S1. Potentially, this positive response in the CNS can be attributed to the inhibition of peripheral cold receptor activity produced by warmth stimulation, which is crucial for warmth perception (Paricio-Montesinos et al., 2020). Altogether, these results indicate that the information of distinct modalities, originally separated in the periphery, later converges, and is integrated into CNS neurons.

Thalamic and cortical OS representation is spatially organized in neuronal clusters

We next studied the spatial distribution of the distinct groups of neurons. For this, we calculated the probability of finding two neurons responding to the same combination of stimuli in the same recording coordinates (P_{near}) and compared it with the overall probability of finding an equal neuron, regardless of recording location (P_{far}) . The ratio between both probabilities allowed us to define the *spatial tuning index*, which indicates how much more probable it is to find two equal-type units in the same recording coordinates vs. in different recording coordinates $(Spatial\ tuning\ index = Pnear/Pfar)$. Spatial tuning indexes for TG units were around 1, indicating no spatial clustering (Fig. 7A). On the contrary, values around 1.5 and 2.5 were obtained for thalamic

and cortical units, respectively (Fig. 7A). Then, to further study spatial organization, the recording coordinates in the three axes (DV, AP, ML) were defined for each neuron. After that, we quantified the distance between the recording coordinates of each pair of neurons and determined whether they were functionally equal (in red) or not (in black, Fig. 7B). The homogeneity of variance test showed that equal-type units are closer in the three axes in S1, while in TG and Th, functionally similar units are only organized in AP axes (Fig 7B). Taken together, these results indicate that the functional spatial organization of OS-responsive neurons evolves along the pathway, from a low spatial organization in the TG, increased in Th, and maximized at S1, in which tridimensional clusters of neurons sharing similar sensitivity are formed.

Neuronal spontaneous activity is related to modality sensitivity

Data show that populational spontaneous activity (median spikes/s \pm IQR) was higher in Th (3.9 \pm 4.7), followed by S1 (3 \pm 3.2), while TG showed the lower activity (1.6 \pm 2.1) (S1 vs. Th P = 0.028; S1 vs. TG P = 0.006; Th vs. TG P = 0.001, Bonferroni post hoc comparison).

When considering single neurons, it should be noted that the spontaneous activity of a given neuron depends on its own excitability and the external synaptic inputs that it receives from the circuit in which it is integrated. Following this logic, a CNS neuron responding to cold can present different spontaneous activity from another one not responding to cold, as the first neuron is embedded

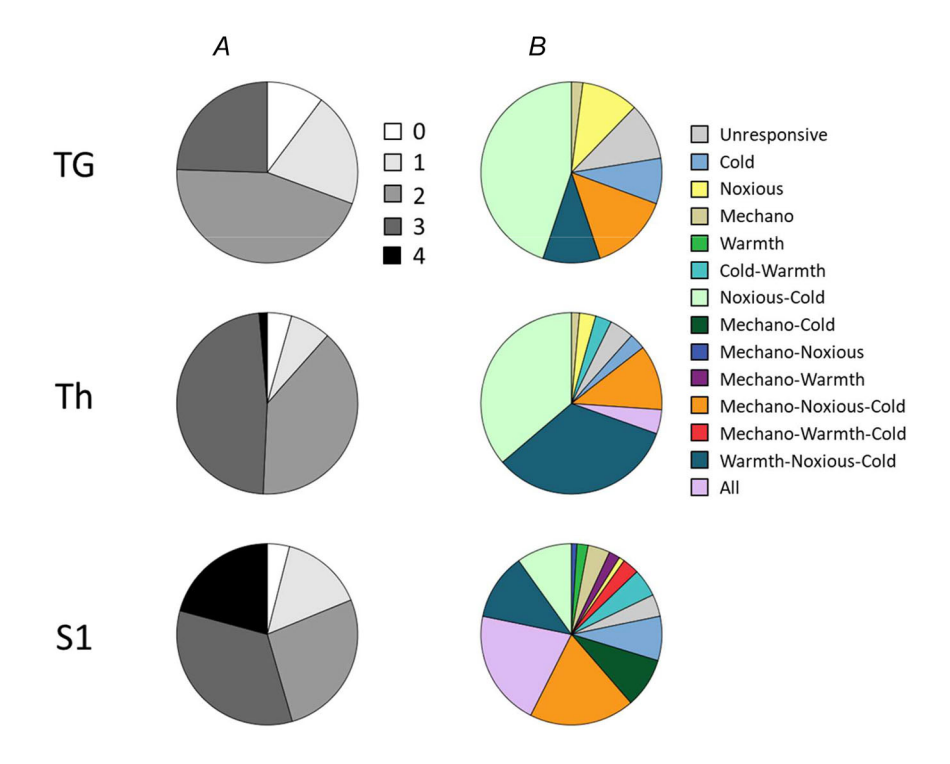


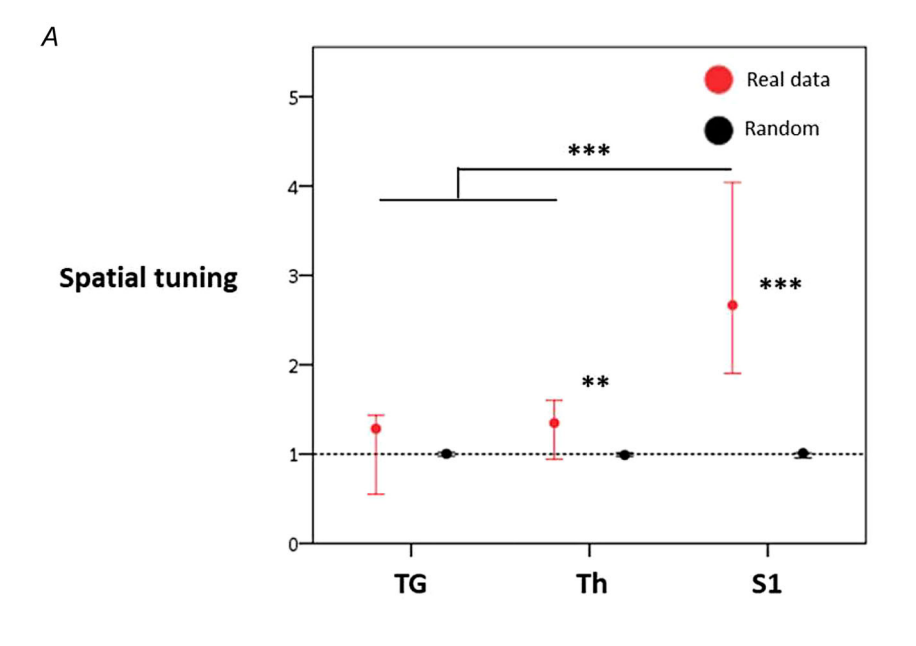
Figure 6. Multimodality and functional diversity of single neurons is increased along the somatosensory pathway

14697793, 2024, 7, Downloaded from https://physoc.onlinelibrary.wiley.com/doi/10.1131/P285080 by Readcube (Labtiva Inc.), Wiley Online Library on [23/05/2024], See the Terms and Conditions (https://olinelibrary.wiley.com/erms-and-conditions) on Wiley Online Library for rules of use; OA arctices are governed by the applicable Creative Commons Licensea

A, percentages of TG, Th and S1 units with different degrees of multimodality, a parameter defined as the number of different types of stimuli a single unit responded to, established between 0 (activated by no stimulus, white) and 4 (activated by all four stimuli, black). B, proportion of single TG, Th and S1 units with positive response to each possible combination of stimuli. Notice that neurons responding to all possible combinations except for Warmth-Noxious and Mechano-Warmth-Noxious were found. N: TG = 49 single units; Th = 69; S1 = 101. Single units were isolated from 17 recording sites in S1, 15 in Th and 8 in TG, from a total of 17 animals. [Colour figure can be viewed at wileyonlinelibrary.com]

14697793, 2024, 7, Downloaded from https://physoc.onlinelibrary.wiley.com/doi/10.1113/JP285008 by Readcube (Labtiva Inc.), Wiley Online Library on [23/05/2024]. See the Terms

conditions) on Wiley Online Library for rules of use; OA articles are governed by the applicable Creative Commons I



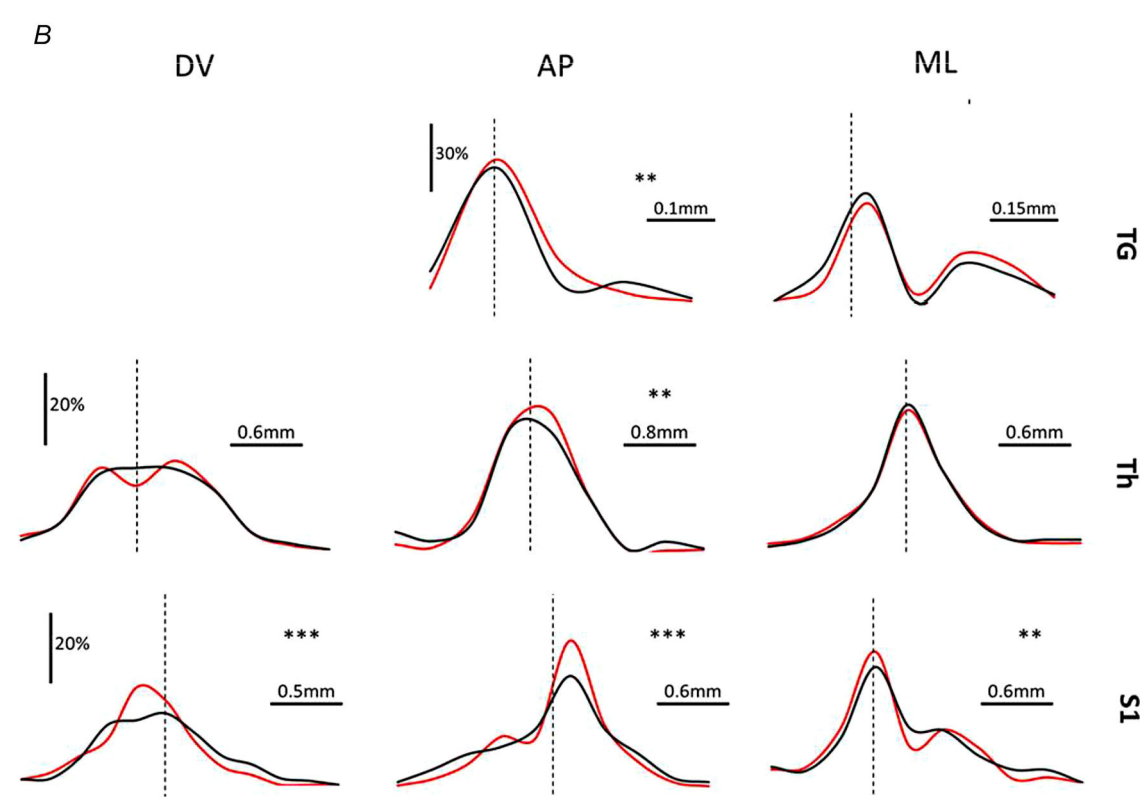


Figure 7. Thalamic and cortical ocular surface representation is spatially organized in neuronal clusters A, spatial tuning index (STI) calculated for units of the same functional type (explanation of the metric in the text). STIs from real data were compared with STIs calculated after units were randomly distributed (data shuffled 100 times). Data are represented as medians \pm CI 95%. **P < 0.01, ***P < 0.001; Mann–Whitney's U test for Data vs. Random, and the Kruskal–Wallis plus post hoc Bonferroni test for comparisons between structures. B, distribution of equal-type units (red lines) and non-equal-type units (black lines). DV axis of TG is not represented because recordings were always performed at 10 mm deep. Dotted line represents coordinate 0. Levene's equality of variance test was used for comparisons, **P < 0.01, ***P < 0.001. N: TG = 49 single units; Th = 69; S1 = 101. Single units were isolated from 17 recording sites in S1, 15 in Th and 8 in TG, from a total of 17 animals. [Colour figure can be viewed at wileyonlinelibrary.com]

in a circuit carrying cold-related information while the other one is not. In fact, it has been described that each functional type of OS innervating peripheral sensory neurons shows different degrees of spontaneous activity (Belmonte et al., 2017; Gallar et al., 1993; González-González et al., 2017), a result confirmed in our *in vivo* data from TG (Fig. 8A). As a consequence, a CNS neuron embedded in the cold circuit is constantly receiving activity from the periphery, while a non-cold-sensing CNS neuron is not. In this sense,

cold-sensitive neurons have higher spontaneous activity than non-cold-sensitive neurons, in TG and Th, but not in S1 (Fig. 8B). Interestingly, noxious heat-sensitive neurons show higher activity than noxious-unresponsive units in Th and S1 (Fig. 8C). For warmth and mechano-modality circuits there were almost no differences (Fig. 8D–E). Noteworthy, we observed that neurons integrating more modalities of stimuli present higher spontaneous activity in general, both for Th and S1 units (Fig. 8F). These results allow us to propose that neuronal spontaneous activity is

14697793, 2024, 7, Downloaded from https://physoc.onlinelibrary.wiley.com/doi/10.1113/JP285008 by Readcube (Labtiva Inc.), Wiley Online Library on [23/05/2024]. See the Terms

nditions) on Wiley Online Library for rules of use; OA articles are governed by the applicable Creative Commons License

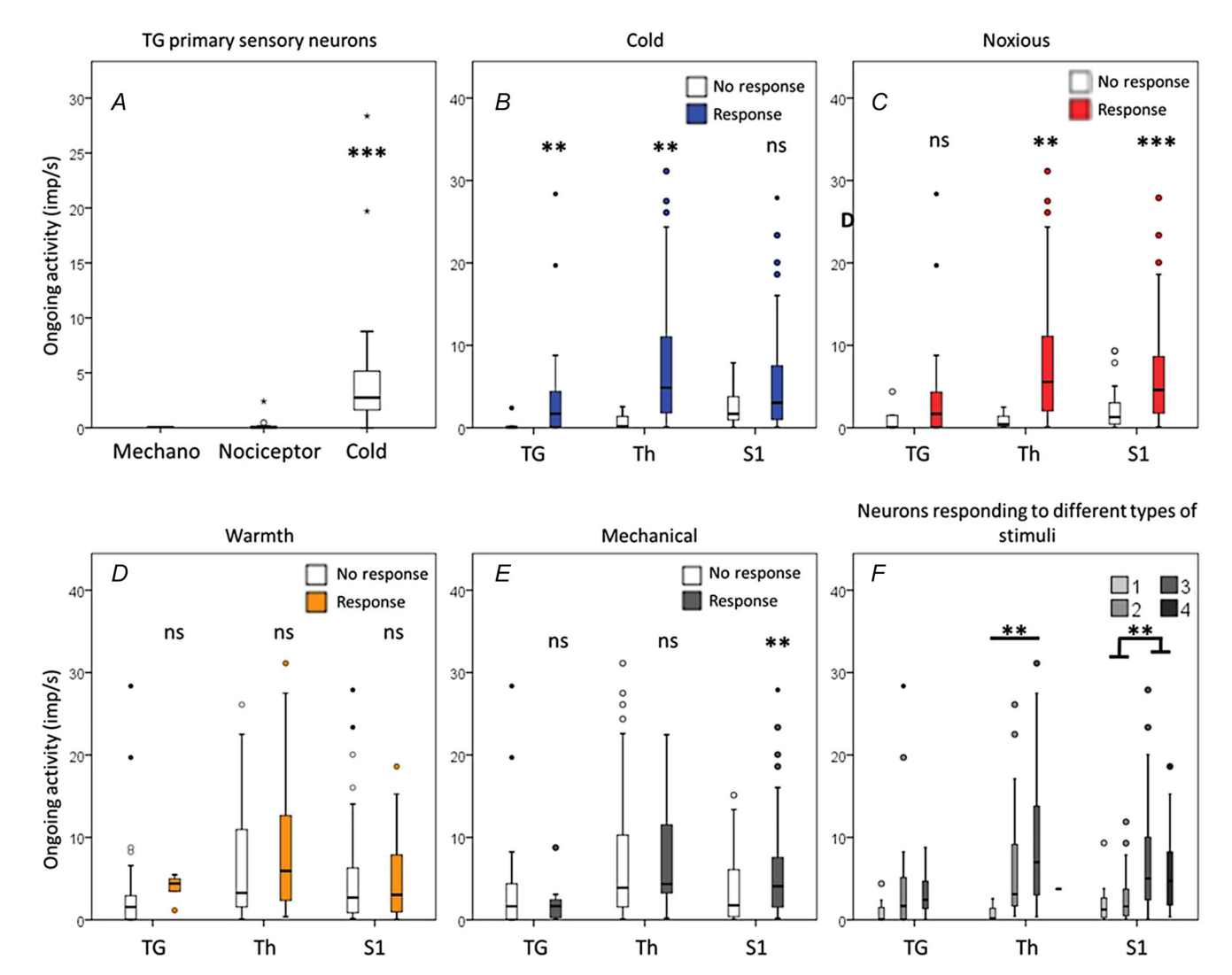


Figure 8. Spontaneous activity of trigeminal, thalamic and S1 units responding or not to different modalities

A, spontaneous activity of TG units responding to ocular surface (OS) stimulation, classified as mechanoreceptor, polymodal nociceptor and cold thermoreceptor neurons, the canonical functional types of OS trigeminal neurons. Mechanoreceptor n=2 single units; Nociceptor n=13; Cold receptor n=29 isolated from 8 TG recordings. B-E, spontaneous activity of OS units recorded in TG, Th and S1. Values of spontaneous activity of the responding neurons to a given modality were compared with the spontaneous activity of non-responding neurons of that modality. F, spontaneous activity of TG, Th and S1 in function of their level of multimodality (see text and Fig. 7 for details on multimodality). F < 0.05; F < 0.01; F < 0.01; F < 0.001, F × = 49 single units; Th = 69; S1 = 101. Single units were isolated from 17 recording sites in S1, 15 in Th and 8 in TG, from a total of 17 animals. [Colour figure can be viewed at wileyonlinelibrary.com]

4997793, 2024, 7, Downloaded from https://physoc.onlinelibrary.wiley.com/doi/10.1113/JP285908 by Readcube (Labtiva Inc.), Wiley Online Library on [23/05/2024]. See the Terms and Conditions (https://onlinelibrary.wiley.com/terms

-and-conditions) on Wiley Online Library for rules of use; OA articles are governed by the applicable Creative Commons Licenso

modulated by the sum of received inputs, pertaining to different sensory modalities.

Discussion

In this work we have studied the neuronal activity in the trigeminal ganglia, thalamus and cortex in response to the stimulation of the OS with different sensory modalities. While data obtained from TG confirm previous works in the field (Hatta et al., 2019; Hirata et al., 2017; Kurose & Meng, 2013; Robbins et al., 2012), this work provides the first anatomical and physiological characterization of Th and S1 neuronal populations involved in OS sensory processing. However, our data raise many questions that should be discussed in the light of previous research, as well as others that may be the subject of future research to better comprehend the thalamocortical circuits implied in the processing of OS somatosensory information.

Functional representation of the OS at thalamic and cortical level

The thalamocortical somatosensory representation of the whiskers (Chapin & Lin, 1984; Clemens et al., 2018; Deschênes et al., 2005; Furuta et al., 2009; Urbain & Deschênes, 2007), trunk and extremities (Diamond, Armstrong-James, Budway et al., 1992; Diamond, Armstrong-James, Ebner et al., 1992) are pretty well known, but the OS has been almost neglected until now. The brainstem constitutes an exception, as solid works have reported OS representation mainly in the spinal nucleus of the trigeminus, SpV (Marfurt, 1981; Meng et al., 1997; Pozo & Cervero, 1993). In the thalamus, OS and periocular representation coordinates have been reported in the cat (Yokota et al., 1985), and eyebrow guard hair has been recorded in rats (Diamond, Armstrong-James, Budway et al., 1992; Diamond, Armstrong-James, Ebner et al., 1992). Indeed, the anatomical representations of the OS in the thalamus and S1 reported in this work are consistent with previously described somatotopic arrangement of the body and face, as they form a logical continuum with other parts of the face at the coordinates where they are expected, close to the alpha whisker and the first spinal cord level representations.

In the past, most works studying thalamocortical properties of the trigeminal sensory system used tactile stimulation as the main tool to identify neuronal receptive fields, and this can explain why it was easy to find responses to eyebrow guard hairs and eyelid stimulation before, but not to corneal surface. Here, we changed the paradigm of stimulation from tactile to thermal stimulation, following the same rationale as previous studies in the TG and brainstem, and this has been key to unveiling thalamocortical OS responses. To

the best of our knowledge, there has not been a previous report of OS functional responses in S1, except for a case report in a human, in which the authors report pain-related activation of S1 using fMRI (Moulton et al., 2012). Therefore, our results are innovative and coherent with previously described somatotopic organization (Chapin & Lin, 1984), though we cannot rule out other possible coordinates in which OS-responsive neurons could be found.

Functional profiles of the OS neuronal populations along the somatosensory pathway

Here we report that populational responses to OS stimulation displayed two components in the Th and S1. The first component amplitude and latency were not influenced by the temperature of the drop, and its latency was coincident with the fastest innervation of the OS, the A δ mechanical nociceptors. Moreover, the warming stimulus evoked only this first fast component, as no warmth receptors have identified in the cornea (Gallar et al., 1993; González-González et al., 2017). Therefore, we interpreted this first component as the mechanical response towards the saline drop contacting the OS. Meanwhile, the second component was slower, showing a latency in the C-fibre CV range. Interestingly, even when the second component is always within the C-fibre range, its latency showed differences depending on the sensory modality of stimulation. In fact, it was faster for cold stimulation than for noxious heating, matching the CVs of the peripheral receptors detecting each stimulation modality (Fowler et al., 1988).

At the single neuron level, three types of response dynamics were identified: (1) biphasic neurons showing the same response structure as MUA, which presented both an initial (first) and second component, (2) neurons which only contributed to the first initial $A\delta$ mechanical response, and (3) neurons which only contribute to the second, C thermal, component. Interestingly, single-unit analysis revealed that a single neuron can present one type of response dynamic to one type of stimulation and not to another modality. For example, a given cell when stimulated with a cold drop can present only with the first component, indicating that it is receiving mechanical but not cold-related information. Then this same cell when stimulated with noxious heat can respond with both the first and second component, indicating that it is encoding both mechanical and noxious stimulation, as a WDR neuron.

Regarding thermal and noxious stimulation, both noxious heating and cold responses were characterized by a second long-lasting component coincident with C-fibre evoked responses. Indeed, our S1 latencies towards this component matched previously reported latencies

(\sim 200 ms) for thermal responses recorded through MEG and EEG in humans (Fardo et al., 2017; Jin et al., 2018; Wang et al., 2016). Furthermore, its latencies and duration are coherent with cortical synaptic inputs measured intracellularly in vivo in mice (Bokiniec et al., 2018; Milenkovic et al., 2014). Interestingly, mild and intense cold stimulation produced similar responses differing only in their amplitude, while warming and noxious stimulus produced qualitatively different responses. Accordingly, other authors propose that cold intensity is codified as a linear increase in activity both in peripheral (Yarmolinsky et al., 2016) and spinal dorsal horn neurons (Ran et al., 2016). On the contrary, noxious heat responses are differentiated from non-noxious responses by a discrete threshold that activates a differentiated population of nociceptors (Vandewauw & Voets, 2016), which indicates that these two types of stimulation are different sensory modalities. Our results suggest that this thermosensitivity model is also extensible to OS thalamocortical processing. Furthermore, thalamic responses against noxious heat stimulation were strikingly long lasting, and new neurons were being recruited into the response as late as 600 ms after stimulation, outlasting the latencies expected for the slower peripheral fibres. We consider that this long-lasting 'post-discharge' activation during the Th response after nociceptive stimulation could be due to noxious-driven cholinergic action, as it has been previously described in Castro et al. (2017). Moreover, the fact that new units are being recruited during this post-discharge is also consistent with a cholinergic general activation (Castro-Alamancos, 2004; Castro-Alamancos & Oldford, 2002). Another possibility to explain this finding is that activity is reverberating either in the Th local circuit or that a top-down projection from a cortical area is activating the thalamic units. Although less noticeable, thalamic responses to cold were also longer-lasting than cortical responses, maybe due to higher cortical inhibitory activity (Adesnik & Scanziani, 2010; Meyer et al., 2011; Pluta et al., 2019).

A particularly interesting result is the location of OS responding cells in the Th. Stereotaxic coordinates correspond to locations distributed in the dorsolateral border between POm/VPM, including both nuclei. If these recording sites being distributed in both nuclei correspond to the biological reality or are due to individual anatomical differences between animals and the atlas lies beyond the accuracy of the measurement undertaken here. Moreover, POm and VPM present a specular arrangement of their somatotopic representation of the body (Bureau et al., 2006; Diamond, Armstrong-James, Budway et al., 1992; Diamond, Armstrong-James, Ebner et al., 1992). Therefore, it is to be expected that both sides of the VPM-POm border have an OS representation and the only way for us to distinguish whether a recording pertained to POm or VPM is interpreting the functional features of the responses. In this regard, latencies of our recorded mechanical responses were slower than those produced by whisker stimulation in the lemniscal pathway involving VPM (Minnery & Simons, 2003; Minnery et al., 2003; Plomp et al., 2014). Indeed, paralemniscal pathway latencies for mechanical responses in POm (10-30 ms) closely resemble our reported latencies in the thalamus (19-22 ms), in contrast to fast VPM lemniscal responses (4-6 ms) (Aguilar et al., 2008; Diamond, Armstrong-James, Ebner et al., 1992). In this sense, it has been previously reported that mechanosensitive neurons of the OS are slow-conducting nociceptors (Acosta, Belmonte et al., 2001; Belmonte et al., 1991, 2017; Gallar et al., 1993). Considering that corneal innervation is not myelinated (Müller et al., 2003) and subsequently the CVs of OS afferents fall within the A δ -C range (López de Armentia et al., 2000), a low conduction velocity can be expected for information reaching both POm and VPM. In this same line, it has been demonstrated that corneal afferents enter the CNS through the Sp5, the first nuclei in the paralemniscal pathway involving the POm (Marfurt, 1981) and nociceptive information is classically considered to be conveyed through the POm (Mo et al., 2017). However, it is important to note that a direct innervation from SP5 to whisker barreloids in VPM has been described (Veinante et al., 2000), which opens the possibility for the OS pathway to reach both POm and VPM at the same time. Therefore, as our results show consistently neuronal responses in the border of POm-VPM, we consider that the paralemniscal pathway with origin in SP5 could explain responses recorded in both POm and VPM nuclei. Thus, the common inputs from SP5 to POm and VPM could explain the overlap observed in the range of coordinates obtained in our recordings from both thalamic structures (Fig. 2C).

4697793, 2024, 7, Downloaded from https://physoc.onlinelibrary.wiley.com/doi/10.1131P285086 by Readcube (Labitva Inc.), Wiley Online Library or [2305/2024], See the Terms and Conditions (https://onlinelibrary.wiley.com/terms-and-conditions) on Wiley Online Library for rules of use; OA article are governed by the applicable Creative Commons Licensen

In conclusion, functional features of OS-responsive VPM-POm neurons resemble the ones described for the paralemniscal pathway involving mainly the POm, and in a different manner the VPM. Further experiments, such as combined intracellular dying and recording using neurobiotin, should clarify the pathway through which OS information is ascending to the cortex.

Another interesting point to discuss is that, although very few and consequently not contributing to MUA recordings, there are neurons in the Th and S1 presenting positive thermal responses to warmth stimulation. How is this possible if there are no warmth receptors in the OS? Recently, it has been demonstrated that the inhibition of cold receptors, driven by temperature increase, is necessary for warmth perceptions to be produced, and that warmth receptors are not necessary for this to happen (Paricio-Montesinos et al., 2020). Consequently, a tempting hypothesis is that warmth-responsive cells in the CNS are being activated by the inhibition of cold receptors in the periphery. It will be very relevant to test this by

14697793, 2024, 7, Downloaded from https://physoc.onlinelibrary.wiley.com/doi/10.1113/JP285008 by Readcube (Labtiva Inc.), Wiley Online Library on [23/05/2024]. See the Terms

onditions) on Wiley Online Library for rules of use; OA articles are governed by the applicable Creative Commons I

characterizing the response of these warmth-sensitive cells in the CNS to selective inhibition and activation of peripheral cold receptors; for example, through the use of optogenetics.

Multimodal integration in the ocular surface somatosensory pathway

Peripheral innervation of OS is composed by neurons responding to one to three different modalities (Bech et al., 2018; Gallar et al., 1993; González-González et al., 2017), as our results confirmed. To go one step further in the knowledge of sensory processing of OS, we wanted to know how modality of the stimulus is represented at thalamic and cortical level. In this regard, the percentage of neurons responding to three and four modalities was increased in thalamus and cortex, as well as the number of neuronal populations showing distinct combinations of modalities. Furthermore, neurons responding to the same combination of modalities were grouped together in spatial clusters, both in the thalamus and in the cortex. Figure 9 displays a simple conceptual representation of this process.

Whether these functional clusters are determined by common afferent projections (Casas-Torremocha et al., 2019) or by local connectivity remains an open question. The anteroposterior axis is the only one in which TG and Th neurons were organized, while S1 units were organized in the three spatial axes, with the DV axis being predominant. This finding in TG is not surprising, as moving in the ML quickly takes the electrode outside the ophthalmic branch, no longer representing OS (Launay et al., 2015), and moving in the DV axis either takes out the electrode of the TG (dorsal) or crushes it towards the skull (ventral). In Th, this result is coincident with the AP organization of noxious, non-noxious and WDR units innervating the cats' faces reported by (Yokota et al., 1985). In S1, the strong influence of the DV axis could be attributed to the different afferents received by each cortical layer (Mo et al., 2017): the differing projections of the lemniscal (layer IV) and paralemniscal (layers I and V) pathways to S1 could be conferring spatially distributed multimodality along the DV axis (Sherman, 2017). An interesting approach to better characterize this cortical spatial organization would be using high-density electrophysiological recordings and functional imaging.

Altogether, these results reveal that the 'labelled' separated peripheral pathways are integrated into CNS units in a spatially organized way. This has been barely explored in other works, probably due to a bias towards exploring mainly the whisker system, and preferentially use a single stimulation modality consisting in tactile stimulus. Trying to give a functional interpretation of our results, we suggest that the low grade

of complexity regarding multimodal integration of TG neurons is intended to produce early protective responses through clearly defined physiological reflexes. By contrast, increased complexity found at the thalamus and cortex provides the possibility to decipher the nature of stimulus to create a multimodal perception.

Neuronal spontaneous activity relates to the modality sensitivity of the neurons

Spontaneous activity (spontaneous firing of single units) emerges from the local neuronal network of each brain structure through a combination of intrinsic properties of neurons, excitatory and inhibitory input balance, as well as from the action of neuromodulators. Moreover, afferent

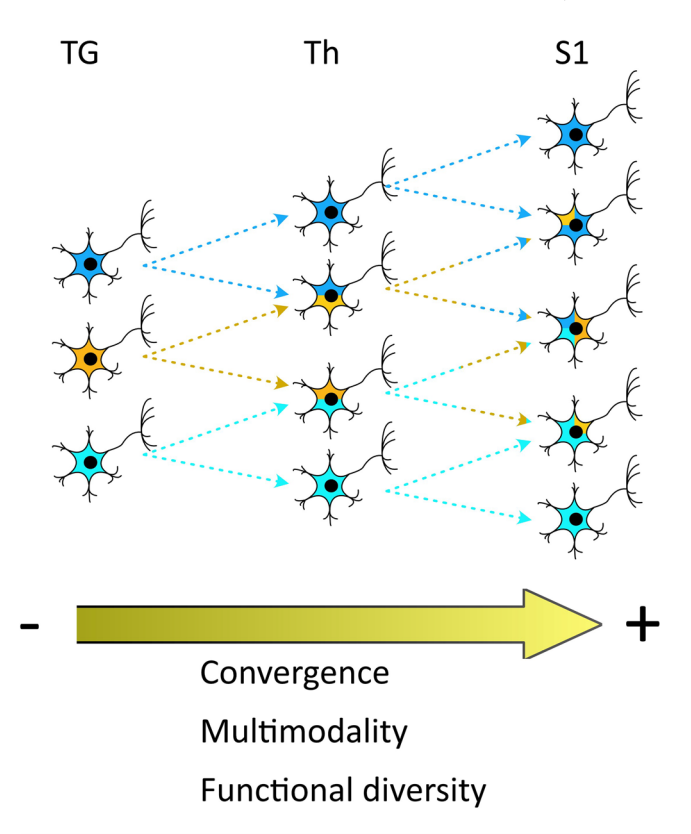


Figure 9. Conceptual model of multimodal integration into single units along the somatosensory axis

Our interpretation is that both divergence and convergence are produced along the pathway from the periphery to the primary sensory cortex (S1) in the central nervous system. Information initially segregated by trigeminal neurons with responsiveness to a specific set of stimulus modalities is being integrated when converging over single neurons (mixed colour neurons) at higher levels of the CNS. Therefore, multimodality is being increased along the pathway, as well as the functional diversity of the neurons, creating spatial clusters with similar functional profiles that integrate almost any possible combination of stimuli. This figure and the colour code displayed on it does not intend to be realistic or match the data, but only to provide a simplified schematic representation of our proposed conceptual model. [Colour figure can be viewed at wileyonlinelibrary.com]

inputs play an important role in determining spontaneous activity, as interruption of ascending pathways or peripheral deafferentation demonstrate (Aguilar et al., 2010; Alonso-Calviño et al., 2016; Bishop & Zito, 2013; Fernández-López et al., 2019; Hengen et al., 2013; Teichert et al., 2017; Zaforas et al., 2021). This notion is further strengthened by our results, as neurons sensitive to more modalities of stimulation display higher spontaneous activity than less polymodal ones. This can contribute to the understanding of how chronic unbalanced activity in the peripheral receptors innervating the OS (due to tissular damage or other pathological conditions) can modulate CNS activity.

Conclusion

Our work describes the somatotopic representation of the OS in the CNS somatosensory structures as thalamus and primary somatosensory cortex. Moreover, we have characterized the physiology of OS sensory processing at populational and single neuron levels, showing the consistency between them, as well as the diversity of neuronal identities in response to different sensory modalities. These findings are crucial for the field of ophthalmology, in which a myriad of highly prevalent somatosensory alterations are poorly understood at the mechanistic level. OS pathologies are presumably producing relevant (and unknown) plastic changes in the thalamocortical circuits, such as those reported for dry eye disease in the brainstem.

Furthermore, we pinpoint some new insights into modality information processing in a highly polymodal tissue like the OS, proposing new principles of organization that are potentially crucial for our understanding of how a unified, multimodal conscious perception is generated. Whether these results are generalizable for all S1 represented structures is a question still to be addressed.

Limitations

In addition to previously mentioned limitations, we want to highlight that the limbus and the conjunctiva of the rats are almost not exposed to the external environment, so we are preferentially stimulating the cornea in this work. Furthermore, we have tried a limited set of stimulus modalities, and others could appear to be relevant for the OS field, such as pure mechanical pressure, acid, osmolarity and dryness stimulation.

References

Acosta, M. C., Belmonte, C., & Gallar, J. (2001). Sensory experiences in humans and single-unit activity in cats evoked by polymodal stimulation of the cornea. *The Journal of Physiology*, **534**(2), 511–525.

- Acosta, M. C., Luna, C., Quirce, S., Belmonte, C., & Gallar, J. (2014). Corneal sensory nerve activity in an experimental model of UV keratitis. *Investigative Ophthalmology & Visual Science*, **55**(6), 3403–3412.
- Acosta, M. C., Tan, M. E., Belmonte, C., & Gallar, J. (2001). Sensations evoked by selective mechanical, chemical, and thermal stimulation of the conjunctiva and cornea. *Investigative Ophthalmology & Visual Science*, **42**, 2063–2067.
- Adesnik, H., & Scanziani, M. (2010). Lateral competition for cortical space by layer-specific horizontal circuits. *Nature*, **464**(7292), 1155–1160.
- Aguilar, J., Humanes-Valera, D., Alonso-Calviño, E., Yague, J. G., Moxon, K. A., Oliviero, A., & Foffani, G. (2010). Spinal cord injury immediately changes the state of the brain. *The Journal of Neuroscience*, **30**(22), 7528–7537.
- Aguilar, J., Morales-Botello, M. L., & Foffani, G. (2008). Tactile responses of hindpaw, forepaw and whisker neurons in the thalamic ventrobasal complex of anesthetized rats. *European Journal of Neuroscience*, **27**(2), 378–387.
- Alonso-Calviño, E., Martínez-Camero, I., Fernández-López, E., Humanes-Valera, D., Foffani, G., & Aguilar, J. (2016). Increased responses in the somatosensory thalamus immediately after spinal cord injury. *Neurobiology of Disease*, **87**, 39–49.
- Bech, F., González-González, O., Artime, E., Serrano, J., Alcalde, I., Gallar, J., Merayo-Lloves, J., & Belmonte, C. (2018). Functional and morphologic alterations in mechanical, polymodal, and cold sensory nerve fibers of the cornea following photorefractive keratectomy. *Investigative Ophthalmology & Visual Science*, **59**(6), 2281–2292.
- Belmonte, C., Aracil, A., Acosta, M. C., Luna, C., & Gallar, J. (2004). Nerves and sensations from the eye surface. *The Ocular Surface*, **2**(4), 248–253.

14697793, 2024, 7, Downloaded from https://physoc.onlinelibrary.wiley.com/doi/10.1131/P285080 by Readcube (Labtiva Inc.), Wiley Online Library on [23/05/2024], See the Terms and Conditions (https://olinelibrary.wiley.com/erms-and-conditions) on Wiley Online Library for rules of use; OA arctices are governed by the applicable Creative Commons Licensea

- Belmonte, C., Nichols, J. J., Cox, S. M., Brock, J. A., Begley, C. G., Bereiter, D. A., Dartt, D. A., Galor, A., Hamrah, P., Ivanusic, J. J., Jacobs, D. S., Mcnamara, N. A., Rosenblatt, M. I., Stapleton, F., & Wolffsohn, J. S. (2017). TFOS DEWS II pain and sensation report. *The Ocular Surface*, **15**(3), 404–437.
- Belmonte, C., Gallar, J., Pozo, M. A., & Rebollo, I. (1991). Excitation by irritant chemical substances of sensory afferent units in the cat's cornea. *The Journal of Physiology*, **437**(1), 709–725.
- Bishop, H. I., & Zito, K. (2013). The downs and ups of sensory deprivation: Evidence for firing rate homeostasis in vivo. *Neuron*, **80**(2), 247–249.
- Bokiniec, P., Zampieri, N., Lewin, G. R., & Poulet, J. F. (2018).The neural circuits of thermal perception. *Current Opinion in Neurobiology*, 52, 98–106.
- Bureau, I., Von Saint Paul, F., & Svoboda, K. (2006). Interdigitated paralemniscal and lemniscal pathways in the mouse barrel cortex. *PLoS Biology*, **4**(12), e382.
- Casas-Torremocha, D., Porrero, C., Rodriguez-Moreno, J., García-Amado, M., Lübke, J. H. R., Núñez, Á., & Clascá, F. (2019). Posterior thalamic nucleus axon terminals have different structure and functional impact in the motor and somatosensory vibrissal cortices. *Brain Structure and Function*, **224**(4), 1627–1645.

- Castro, A., Raver, C., Li, Y., Uddin, O., Rubin, D., Ji, Y., Masri, R., & Keller, A. (2017). Cortical regulation of nociception of the trigeminal nucleus caudalis. *Journal of Neurophysiology*, 37, 11431–11440.
- Castro-Alamancos, M. A., & Oldford, E. (2002). Cortical sensory suppression during arousal is due to the activity-dependent depression of thalamocortical synapses. *The Journal of Physiology*, **541**(1), 319–331.
- Castro-Alamancos, M. A. (2004). Dynamics of sensory thalamocortical synaptic networks during information processing states. *Progress in Neurobiology*, **74**(4), 213–247.
- Chapin, J. K., & Lin, C.-S. (1984). Mapping the body representation in the SI cortex of anesthetized and awake rats. *Journal of Comparative Neurology*, **229**(2), 199–213.
- Clemens, A. M., Fernandez Delgado, Y., Mehlman, M. L., Mishra, P., & Brecht, M. (2018). Multisensory and motor representations in rat oral somatosensory cortex. *Scientific Reports*, **8**(1), 13556.
- Deschênes, M., Timofeeva, E., Lavallée, P., & Dufresne, C. (2005). The vibrissal system as a model of thalamic operations. In *Progress in Brain Research*, pp. 31–40. Progress in Brain Research.
- Diamond, M. E., Armstrong-James, M., & Ebner, F. F. (1992). Somatic sensory responses in the rostral sector of the posterior group (POm) and in the ventral posterior medial nucleus (VPM) of the rat thalamus. *Journal of Comparative Neurology*, **318**(4), 462–476.
- Diamond, M. E., Armstrong-James, M., Budway, M. J., & Ebner, F. F. (1992). Somatic sensory responses in the rostral sector of the posterior group (POm) and in the ventral posterior medial nucleus (VPM) of the rat thalamus: Dependence on the barrel field cortex. *Journal of Comparative Neurology*, **319**(1), 66–84.
- Fakih, D., Zhao, Z., Nicolle, P., Reboussin, E., Joubert, F.,
 Luzu, J., Labbé, A., Rostène, W., Baudouin, C., Mélik
 Parsadaniantz, S., & Réaux-Le Goazigo, A. (2019).
 Chronic dry eye induced corneal hypersensitivity, neuro-inflammatory responses, and synaptic plasticity in the mouse trigeminal brainstem. *Journal of Neuroinflammation*, 16(1), 268.
- Fardo, F., Vinding, M. C., Allen, M., Jensen, T. S., & Finnerup, N. B. (2017). Delta and gamma oscillations in operculo-insular cortex underlie innocuous cold thermosensation. *Journal of Neurophysiology*, 117(5), 1959–1968.
- Fernández-López, E., Alonso-Calviño, E., Humanes-Valera, D., Foffani, G., & Aguilar, J. (2019). Slow-wave activity homeostasis in the somatosensory cortex after spinal cord injury. *Experimental Neurology*, **322**, 113035.
- Fowler, C. J., Sitzoglou, K., Ali, Z., & Halonen, P. (1988). The conduction velocities of peripheral nerve fibres conveying sensations of warming and cooling. *Journal of Neurology, Neurosurgery, and Psychiatry*, **51**(9), 1164–1170.
- Friedberg, M. H., Lee, S. M., & Ebner, F. F. (1999). Modulation of receptive field properties of thalamic somatosensory neurons by the depth of anesthesia. *Journal of Neuro-physiology*, **81**(5), 2243–2252.
- Furuta, T., Kaneko, T., & Deschênes, M. (2009). Septal neurons in barrel cortex derive their receptive field input from the lemniscal pathway. *Journal of Neuroscience*, 29(13), 4089–4095.

- Gallar, J., Acosta, M. C., Moilanen, J. A. O., Holopainen, J. M., Belmonte, C., & Tervo, T. M. T. (2004). Recovery of corneal sensitivity to mechanical and chemical stimulation after laser in situ keratomileusis. *Journal of Refractive Surgery*, **20**(3), 229–235.
- Gallar, J., Pozo, M. A., Tuckett, R. P., & Belmonte, C. (1993). Response of sensory units with unmyelinated fibres to mechanical, thermal and chemical stimulation of the cat's cornea. *The Journal of Physiology*, **468**(1), 609–622.
- Golan, O., & Randleman, J. B. (2018). Pain management after photorefractive keratectomy. *Current Opinion in Ophthalmology*, **29**(4), 306–312.
- González-González, O., Bech, F., Gallar, J., Merayo-Lloves, J., & Belmonte, C. (2017). Functional properties of sensory nerve terminals of the mouse cornea. *Investigative Ophthalmology & Visual Science*, **58**(1), 404–415.
- Guerrero-Moreno, A., Baudouin, C., Melik Parsadaniantz, S., & Réaux-Le Goazigo, A. (2020). Morphological and functional changes of corneal nerves and their contribution to peripheral and central sensory abnormalities. *Frontiers in Cellular Neuroscience*, **14**, 610342.
- Hatta, A., Kurose, M., Sullivan, C., Okamoto, K., Fujii, N., Yamamura, K., & Meng, I. D. (2019). Dry eye sensitizes cool cells to capsaicin-induced changes in activity via TRPV1. *Journal of Neurophysiology*, **121**(6), 2191–2201.
- Hengen, K. B., Lambo, M. E., Van Hooser, S. D., Katz, D. B., & Turrigiano, G. G. (2013). Firing rate homeostasis in visual cortex of freely behaving rodents. *Neuron*, **80**(2), 335–342.
- Hirata, H., Mizerska, K., Dallacasagrande, V., & Rosenblatt, M. I. (2017). Estimating the osmolarities of tears during evaporation through the "eyes" of the corneal nerves. *Investigative Ophthalmology & Visual Science*, **58**(1), 168–178.
- Jin, Q. Q., Wu, G. Q., Peng, W. W., Xia, X. L., Hu, L., & Iannetti, G. D. (2018). Somatotopic representation of second pain in the primary somatosensory cortex of humans and rodents. *Journal of Neuroscience*, 38(24), 5538–5550.
- Kasetsuwan, N., Satitpitakul, V., Changul, T., & Jariyakosol, S. (2013). Incidence and pattern of dry eye after cataract surgery. *PLoS ONE*, **8**(11), e78657.
- Kato, K., Miyake, K., Hirano, K., & Kondo, M. (2019). Management of postoperative inflammation and dry eye after cataract surgery. *Cornea*, **38**(1), S25–S33.
- Kovács, I., Luna, C., Quirce, S., Mizerska, K., Callejo, G.,
 Riestra, A., Fernández-Sánchez, L., Meseguer, V. M.,
 Cuenca, N., Merayo-Lloves, J., Acosta, M. C., Gasull, X.,
 Belmonte, C., & Gallar, J. (2016). Abnormal activity of corneal cold thermoreceptors underlies the unpleasant sensations in dry eye disease. *Pain*, 157(2), 399–417.
- Kurose, M., & Meng, I. D. (2013). Dry eye modifies the thermal and menthol responses in rat corneal primary afferent cool cells. *Journal of Neurophysiology*, **110**(2), 495–504.
- Launay, P.-S., Godefroy, D., Khabou, H., Rostene, W., Sahel, J.-A., Baudouin, C., Melik Parsadaniantz, S., & Reaux-Le Goazigo, A. (2015). Combined 3DISCO clearing method, retrograde tracer and ultramicroscopy to map corneal neurons in a whole adult mouse trigeminal ganglion. *Experimental Eye Research*, **139**, 136–143.

- López De Armentia, M., Cabanes, C., & Belmonte, C. (2000). Electrophysiological properties of identified trigeminal ganglion neurons innervating the cornea of the mouse. *Neuroscience*, **101**(4), 1109–1115.
- Luna, C., Mizerska, K., Quirce, S., Belmonte, C., Gallar, J., Acosta, M. D. C., & Meseguer, V. (2021). Sodium channel blockers modulate abnormal activity of regenerating nociceptive corneal nerves after surgical lesion. *Investigative Ophthalmology & Visual Science*, **62**(1), 2.
- Marfurt, C. F. (1981). The somatotopic organization of the cat trigeminal ganglion as determined by the horseradish peroxidase technique. *Anatomical Record*, **201**(1), 105–118.
- Meacham, K., Shepherd, A., Mohapatra, D. P., & Haroutounian, S. (2017). Neuropathic pain: Central vs. peripheral mechanisms. *Current Pain and Headache Reports*, **21**(6), 28.
- Meng, I. D., Hu, J. W., Benetti, A. P., & Bereiter, D. A. (1997). Encoding of corneal input in two distinct regions of the spinal trigeminal nucleus in the rat: Cutaneous receptive field properties, responses to thermal and chemical stimulation, modulation by diffuse noxious inhibitory controls, and projections to the p. *Journal of Neuro-physiology*, 77(1), 43–56.
- Meyer, H. S., Schwarz, D., Wimmer, V. C., Schmitt, A. C., Kerr, J. N. D., Sakmann, B., & Helmstaedter, M. (2011). Inhibitory interneurons in a cortical column form hot zones of inhibition in layers 2 and 5A. Proceedings of the National Academy of Sciences of the United States of America, 108(40), 16807–16812.
- Milenkovic, N., Zhao, W.-J., Walcher, J., Albert, T., Siemens, J., Lewin, G. R., & Poulet, J. F. A. (2014). A somatosensory circuit for cooling perception in mice. *Nature Neuroscience*, **17**(11), 1560–1566.
- Minnery, B. S., Bruno, R. M., & Simons, D. J. (2003). Response transformation and receptive-field synthesis in the lemniscal trigeminothalamic circuit. *Journal of Neuro-physiology*, **90**(3), 1556–1570.
- Minnery, B. S., & Simons, D. J. (2003). Response properties of whisker-associated trigeminothalamic neurons in rat nucleus principalis. *Journal of Neurophysiology*, **89**(1), 40–56.
- Mo, C., Petrof, I., Viaene, A. N., & Sherman, S. M. (2017). Synaptic properties of the lemniscal and paralemniscal pathways to the mouse somatosensory thalamus. *Proceedings of the National Academy of Sciences of the United States of America*, **114**(30), E6212–E6221.
- Moulton, E. A., Becerra, L., Rosenthal, P., & Borsook, D. (2012). An approach to localizing corneal pain representation in human primary somatosensory cortex. *PLoS ONE*, 7(9), e44643.
- Müller, L. J., Marfurt, C. F., Kruse, F., & Tervo, T. M. T. (2003). Corneal nerves: Structure, contents and function. *Experimental Eye Research*, **76**(5), 521–542.
- Paricio-Montesinos, R., Schwaller, F., Udhayachandran, A., Rau, F., Walcher, J., Evangelista, R., Vriens, J., Voets, T., Poulet, J. F. A., & Lewin, G. R. (2020). The sensory coding of warm perception. *Neuron*, **106**(5), 830–841. e3.e3.

- Parra, A., Madrid, R., Echevarria, D., Del Olmo, S., Morenilla-Palao, C., Acosta, M. C., Gallar, J., Dhaka, A., Viana, F., & Belmonte, C. (2010). Ocular surface wetness is regulated by TRPM8-dependent cold thermoreceptors of the cornea. *Nature Medicine*, **16**(12), 1396–1399.
- Paxinos, G., & Watson, C. (2007). The rat brain in stereotaxic coordinates.
- Piña, R., Ugarte, G., Campos, M., Íñigo-Portugués, A., Olivares, E., Orio, P., Belmonte, C., Bacigalupo, J., & Madrid, R. (2019). Role of TRPM8 channels in altered cold sensitivity of corneal primary sensory neurons induced by axonal damage. *Journal of Neuroscience*, **39**(41), 8177–8192.
- Pinto, V., Derkach, V. A., & Safronov, B. V. (2008). Role of TTX-sensitive and TTX-resistant sodium channels in Adelta- and C-fiber conduction and synaptic transmission. *Journal of Neurophysiology*, **99**(2), 617–628.
- Plomp, G., Quairiaux, C., Kiss, J. Z., Astolfi, L., & Michel, C. M. (2014). Dynamic connectivity among cortical layers in local and large-scale sensory processing. *European Journal of Neuroscience*, **40**(8), 3215–3223.
- Pluta, S. R., Telian, G. I., Naka, A., & Adesnik, H. (2019). Superficial layers suppress the deep layers to fine-tune cortical coding. *Journal of Neuroscience*, 39(11), 2052–2064.
- Pozo, M. A., & Cervero, F. (1993). Neurons in the rat spinal trigeminal complex driven by corneal nociceptors:
 Receptive-field properties and effects of noxious stimulation of the cornea. *Journal of Neurophysiology*, 70(6), 2370–2378.

14697793, 2024, 7, Downloaded from https://physoc.onlinelibrary.wiley.com/doi/10.1131/P285080 by Readcube (Labtiva Inc.), Wiley Online Library on [23/05/2024], See the Terms and Conditions (https://olinelibrary.wiley.com/erms-and-conditions) on Wiley Online Library for rules of use; OA arctices are governed by the applicable Creative Commons Licensea

- Quallo, T., Vastani, N., Horridge, E., Gentry, C., Parra, A., Moss, S., Viana, F., Belmonte, C., Andersson, D. A., & Bevan, S. (2015). TRPM8 is a neuronal osmosensor that regulates eye blinking in mice. *Nature Communications*, **6**(1), 7150.
- Rahman, M., Okamoto, K., Thompson, R., Katagiri, A., & Bereiter, D. A. (2015). Sensitization of trigeminal brainstem pathways in a model for tear deficient dry eye. *Pain*, **156**(5), 942–950.
- Rahman, M., Shiozaki, K., Okamoto, K., Thompson, R., & Bereiter, D. A. (2017). Trigeminal brainstem modulation of persistent orbicularis oculi muscle activity in a rat model of dry eye. *Neuroscience*, **349**, 208–219.
- Ran, C., Hoon, M. A., & Chen, X. (2016). The coding of cutaneous temperature in the spinal cord. *Nature Neuroscience*, **19**(9), 1201–1209.
- Rivera, L., Gallar, J., Pozo, M. A., & Belmonte, C. (2000). Responses of nerve fibres of the rat saphenous nerve neuroma to mechanical and chemical stimulation: An in vitro study. *The Journal of Physiology*, **527**(2), 305.
- Robbins, A., Kurose, M., Winterson, B. J., & Meng, I. D. (2012). Menthol activation of corneal cool cells induces TRPM8-mediated lacrimation but not nociceptive responses in rodents. *Investigative Ophthalmology & Visual Science*, **53**(11), 7034–7042.
- Rossum, G. V., & Drake, F. L. (2009). Introduction to Python 3.

- Sanzarello, I., Merlini, L., Rosa, M. A., Perrone, M., Frugiuele, J., Borghi, R., & Faldini, C. (2016). Central sensitization in chronic low back pain: A narrative review. *Journal of Back and Musculoskeletal Rehabilitation*, 29(4), 625–633.
- Sherman, S. M. (2017). Functioning of circuits connecting thalamus and cortex. *Comprehensive Physiology*, 7, 713–739.
- Teichert, M., Liebmann, L., Hübner, C. A., & Bolz, J. (2017). Homeostatic plasticity and synaptic scaling in the adult mouse auditory cortex. *Scientific Reports*, 7(1), 17423.
- Toda, I. (2018). Dry eye after lasik. *Investigative*Ophthalmology & Visual Science, **59**(14), DES109–DES115.
- Urbain, N., & Deschênes, M. (2007). A new thalamic pathway of vibrissal information modulated by the motor cortex. *Journal of Neuroscience*, **27**(45), 12407–12412.
- Vandewauw, I., & Voets, T. (2016). Heat is absolute, cold is relative. *Nature Neuroscience*, **19**(9), 1188–1189.
- Veinante, P., Jacquin, M. F., & DeschêNes, M. (2000). Thalamic projections from the whisker-sensitive regions of the spinal trigeminal complex in the rat. *Journal of Comparative Neurology*, **420**(2), 233–243.
- Wang, L., Gui, P., Li, L., Ku, Y., Bodner, M., Fan, G., Zhou, Y.-D.i, & Dong, X.-W. (2016). Neural correlates of heat-evoked pain memory in humans. *Journal of Neurophysiology*, **115**(3), 1596–1604.
- Woolf, C. J. (1983). Evidence for a central component of post-injury pain hypersensitivity. *Nature*, **306**(5944), 686–688.
- Yarmolinsky, D. A., Peng, Y., Pogorzala, L. A., Rutlin, M., Hoon, M. A., & Zuker, C. S. (2016). Coding and plasticity in the mammalian thermosensory system. *Neuron*, **92**(5), 1079–1092.
- Yokota, T., Koyama, N., & Matsumoto, N. (1985). Somatotopic distribution of trigeminal nociceptive neurons in ventrobasal complex of cat thalamus. *Journal of Neurophysiology*, **53**(6), 1387–1400.
- Zaforas, M., Rosa, J. M., Alonso-Calviño, E., Fernández-López, E., Miguel-Quesada, C., Oliviero, A., & Aguilar, J. (2021). Cortical layer-specific modulation of neuronal activity after sensory deprivation due to spinal cord injury. *The Journal of Physiology*, **599**(20), 4643–4669.

Additional information

Data availability statement

Available upon request.

Competing interests

All authors declare not to have any conflicts of interest.

Author contributions

E.V., J.A. and J.G. conceptualized the experiments. Experimentation, data curation, visualization, software development and formal analysis were performed by E.V. with the collaboration of M.Z. The original draft was written by E.V. and J.A. M.C.A., J.A. and J.G. supervised and administered the project. All authors reviewed and edited the final version of the manuscript.

Funding

This work was funded by the Spanish Ministry of Science and Innovation MCIN/AEI/10.13039/501 100 011 033 to J.A. (Grant PID2019-105020GB-I00), and grants SAF-2017-83 674-C2-1-R, SAF-2017-83 674-C2-1-2-R and PID2020-115934RB-I00 (to J.G. and M.C.A.) co-funded by 'ERDF A way of making Europe'. Predoctoral fellowships FPU16/00283 from the Spanish Ministry of Universities (E.V.) and BES2017-08 2029 from AEI (M.Z.) co-funded by 'ESF Investing in your future' and the Generalitat Valenciana Excellence Program grant PROMETEO/2018/114 are also acknowledged. Finally, the European Commission MSCA postdoctoral fellowship RIIBS (101 105 721).

Acknowledgements

The authors want to acknowledge the invaluable technical assistance of Carolina Luna, Elena Alonso-Calviño, Elena Fernández-López and Verónica Ferrer Panes. Also, to José María Delgado, as this collaboration was a direct consequence of the interaction between E.V. and J.A. at the National Course in Neuroscience he organizes, which merges and strengthens the relationship between generations of neuroscientists in our country. And to Amparo, who also contributes to this purpose in her own way.

Keywords

central nervous system, cold, multimodality, ocular surface, pain, somatosensory processing, thermosensation

Supporting information

Additional supporting information can be found online in the Supporting Information section at the end of the HTML view of the article. Supporting information files available:

Peer Review History

Translational perspective

Here we characterize, for the first time, the neurons in the primary sensory cortex and thalamus that respond to ocular surface stimulation. This is a milestone for ophthalmology, as it is known that painful diseases modify the central nervous system, contributing to the maintenance and refractoriness of the symptoms. Therefore, the characterization of ocular surface representation of the thalamus and cortex will enable an interrogation of the neural foundation of important diseases such as trigeminal neuralgia and dry eye disease, guiding new therapeutic approaches such as brain stimulation.

Furthermore, we analysed how stimulus of distinct types (modalities) are integrated, from the sensory neurons directly innervating the ocular surface to the thalamus and cortex integrating information. Modality integration in the somatosensory cortex and thalamus has been barely explored, and our contribution here is double: first, we present the ocular surface as an ideal study model, as it is highly sensitive to many modalities and is accessible to stimulation. Secondly, knowing how different modalities are integrated generates a better understanding of analgesia produced by sensory stimulation, such as cold-induced analgesia or touch/compression-induced analgesia. These findings are therefore also relevant for pain medicine and somatosensory neuroscience.

14697793, 2024, 7, Downloaded from https://physoc.onlinelibrary.wiley.com/doi/10.1113/JP285008 by Readcube (Labtiva Inc.), Wiley Online Library on [23/05/2024]. See the Terms